Effects of Starvation on *Matrix-Metalloproteinase 2* Expression in the Larval fat body of *Drosophila melanogaster*

By

Zoe Wolfel

A Paper Presented to the

Faculty of Mount Holyoke College in

Partial Fulfillment of the Requirements for

the Degree of Bachelor of Arts with

Honor

Department of Biological Sciences

South Hadley, MA 01075

April 25, 2024

This paper was prepared

under the direction of

Professor Craig Woodard

for eight credits.

To my Mom,

Who I could not have done this without.

ACKNOWLEDGEMENTS

Firstly, I would like to thank Professor Craig Woodard for mentoring me through my time in the Woodard lab. The opportunity to be a part of this lab has been one of my most valued experiences during my time at Mount Holyoke. Thank you for your constant support and guidance throughout the past three years and for pushing me to be the best I can.

I would also like to thank the Department of Biological Sciences and the Christianna Smith research grant for funding my thesis and providing the resources that allowed me to work on this research project.

Additionally, I would like to thank the other members of my thesis committee Professor Rebeccah Lijek and Professor Kenneth Colodner. Thank you for your support, guidance, and time throughout this process. I would like to thank Justin Baumann for his knowledge of R studios and help with my statistical analysis. I am so grateful for your willingness to help. I would also like to thank Amanda Maciuba for her experience and support in Adobe Illustrator. Thank you for helping me bridge the gap between art and science. Additionally, I would like to thank my family and friends for unwavering support.

Lastly, I would like to thank the members of the Woodard Lab past and present. This lab has fostered such a welcoming environment and been so supportive of my work. This has been such a great experience because of the people in this lab. In particular Madigan Stichter and Andie Hardin for going through the thesis process with me.

TABLE OF CONTENTS

Page

List of Figures

List of Tables

Abstract

Insulin sensitivity declines with age in mammals, leading to diseases such as type 2 diabetes and obesity, yet the precise mechanism is not well understood. The modulation of insulin signaling is implicated in the pathogenesis of the diseases and plays a critical role in various metabolic processes. The matrix-metalloproteinase (MMP) are a family of multifunctional Zn^{2+}-dependent protease enzymes that play a role in tissue development, cell organization, and cell cycle control in mammals and the model organism *Drosophila melanogaster* which are a great model organism for research because it has a rapid life cycle, is small and easily cultured, male and female individuals are easily differentiated, and they share 75% similarity to all human genes implicated in disease. (Guo et al., 2022). Many MMPs are attached to the cell membrane by the protein glycosylphosphatidylinositol (GPI), which allows them to interact with the extracellular matrix (ECM). In *Drosophila* there are two MMPs: MMP1 and MMP2 which together degrade ECM components (Jia et al., 2014). I investigated the role of MMPs in the regulation of insulin signaling.

Past studies have examined the indirect involvement of *Drosophila* MMP2 in insulin signaling (Bond, 2010). Along with a homolog for MMP2, MMP14 direct cleavage of insulin receptor in a murine model, consequently suppressing insulin signaling. In my investigation, I studied the role of MMP2 in insulin signaling during larval development by performing starvation experiments. I hypothesize that starvation induces *MMP2* expression to allow MMP2 to cleave insulin receptor, which shuts off insulin signaling, allowing autophagy and nutrient release to occur. In order to test this hypothesis I have examined *MMP2* transcript levels in the fat bodies of fed and starved third instar larvae using real time quantitative Polymerase Chain Reaction (PCR). The results of my experiments support my hypothesis that higher *MMP2* transcript levels are observed in a starved condition compared to a fed control.

INTRODUCTION

Summary

The risk of specific cancers increases in patients with obesity, diabetes, and other types of metabolic dysfunction. Cancer metastasis is characterized by the migration of tumor cells to tissue that was previously unaffected. *Drosophila melanogaster*, commonly called the fruit fly, is a well studied system for research. During fat body remodeling, *Drosophila melanogaster* fat body cells mirror behavior similar to metastasizing tumor cells (Hirabayashi et al., 2013; Papalexi, 2013). Using *Drosophila melanogaster* as a model we can explore the relationship between insulin signaling and fat body remodeling.

Type Two Diabetes and Metabolic Dysfunction

90% of diabetes is accounted for by type 2 diabetes mellitus (T2DM). Diabetes mellitus is characterized by persistent hyperglycemia. In T2DM, the response to insulin is diminished. This is defined as insulin resistance (Goyal et at., 2023). T2DM is most common in people over 45, and age is associated with increased insulin resistance (Goyal et al., 2023; Guo et al., 2023). The development of insulin resistance causes an inability of cells to take up circulating glucose. The increase in blood sugar can put stress on an individual's pancreas and liver (Freeman et al., 2023). Currently treatments mostly include managing

diet, and exercising (Goyal et al., 2023). It is important to find therapeutics that target increased insulin sensitivity. This becomes more pressing as insulin becomes less accessible due to its rise in price. Millions of people around the world rely on insulin treatments for their survival. Studying insulin signaling and its inhibitors has the potential to aid in finding new therapeutic targets.

Insulin and Insulin Signaling

Insulin is a circulating anabolic hormone, which is a growth hormone. Insulin is essential in tissue development of insulin dependent cells such as adipose tissue, liver, and muscles, growth, and maintenance of glucose homeostasis in organisms including mammals and insects like the model organism *Drosophila melanogaster*. Insulin is part of a superfamily of insulin-like peptides (ILPs) derived from a ubiquitous genetic group found across vertebrates and mollusks, insects, and nematodes (Biglou et al., 2021). Insulin signaling is an evolutionarily conserved pathway that is found in many organisms including insects, like *Drosophila*, and mammals, like mice and humans, that use it to regulate their growth and metabolic processes. In humans, diseases such as type 2 diabetes, high blood pressure, and other metabolic dysfunction increase when insulin signaling fails to effectively regulate growth and metabolism. This signaling pathway is regulated by insulin-like peptides (ILPs) which bind to and control the activity of their respective receptor (Semanik et al., 2018). This

regulation happens by the binding of insulin or other ILPs, such as insulin growth factor 1 and insulin growth factor 2 (IGF-I & IGF-II), that bind to the transmembrane protein called insulin receptor (InR). In humans, human insulin receptor (hINR) is closely related to insulin-like growth factor receptor in *Drosophila*; they are both members of the tyrosine kinase receptor family (Figure 1) (Biglou et al., 2021).

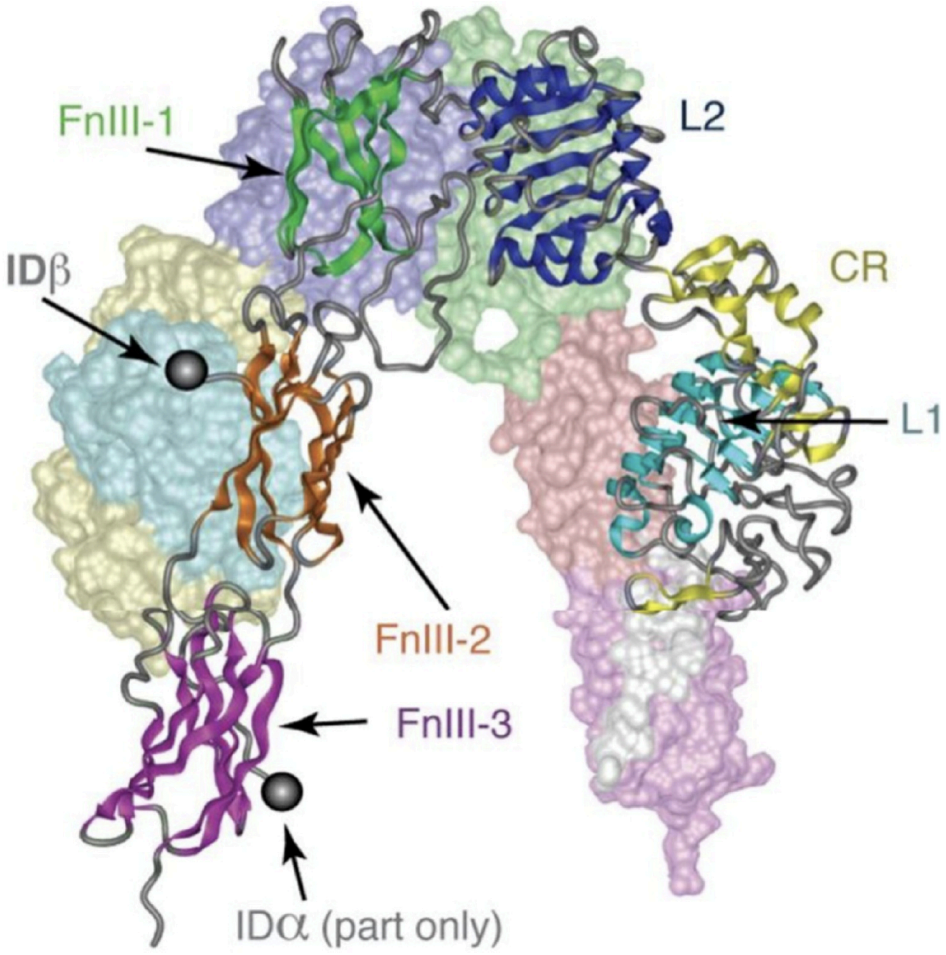

Figure 1. Crystal Structure of the Ectodomain of the Human Insulin Receptor. Structure derived from X-ray crystallization of the receptor. One monomer is depicted in the secondary structure, the alternate receptor monomer in the 3D, surface representation. The grey spheres represent the observed C terminus of the α-chain (IDα) and the observed N terminus of the β-chain (IDβ). L1 and L2 in the figure refer to the two leucine-rich repeats. In humans hINR is closely related to insulin-like growth factor receptor in *Drosophila*, they are both members of the tyrosine kinase receptor family (Figure from Biglou et al., 2021).

Insulin Signaling Across Different Taxa

In mammals such as humans insulin signaling is associated with glucose homeostasis. hINR is critical for regulation of glycogen storage and fat metabolism in the body. The insulin receptor (hINR) is essential for regulating glycogen storage and fat metabolism. When insulin-like peptides (ILPs) bind to the insulin receptor (InR), it triggers conformational changes that lead to the autophosphorylation of tyrosine residues on the receptor. These phosphorylated residues serve as binding sites for various signaling proteins, such as insulin receptor substrate (IRS), initiating downstream signaling cascades within the cell. The catalytic subunit of phosphatidylinositol 3-kinases (PI3K) is recruited upon the binding of IRS1 and -2 to the non-catalytic PI3K subunits. This recruitment activates PI3K, resulting in the production of the minor acidic phospholipid product, phosphatidylinositol-triphosphate (PIP3). However, this step is counteracted by the PTEN phosphatase, which converts PIP3 back to phosphatidylinositol 4,5-bisphosphate (PIP2). The production of PIP3 subsequently activates AKT/PKB (protein kinase B) through phosphoinositide-dependent protein kinase 1 and -2 (PDKs). AKT/PKB activation inhibits the forkhead box-containing protein, O subfamily (FOXO), by sequestering it outside the nucleus. FOXO is a transcription factor that regulates the expression of various genes, including phosphoenolpyruvate carboxykinase

(PEPCK), an important enzyme in gluconeogenesis. Therefore, AKT/PKB activation ultimately results in the inhibition of FOXO and subsequent regulation of gene expression (Biglou et al., 2021).

Insulin Signaling in *Drosophila*

The Insulin-Like Growth Factor Signaling (IIS) pathway also referred to as the insulin signaling pathway is initiated by the binding *Drosophila* insulin-like peptide (dILP) activation via autophosphorylation of the receptor (Figure 2) (Biglou et al., 2021; Semanik et al., 2018). Mammalian insulin has many structural and functional similarities to dILPs (Semanik et al., 2018). The protein structures are similar enough that mammalian insulin can bind to *Drosophila* Insulin Receptor (dInR) (Taguchi and White, 2008). Individuals without dInR can not survive through the larval stage of development. Eight *Drosophila* insulin-like peptides (dILPs) have been identified, dILP 1-8 (Semanik et al., 2018). dILP 1-8 display cell and stage specific expression patterns. The eight dILPs (dILP1-8) are similar structurally, though the exact function of each of the dILPs (1-8) are not fully understood. While they may not fully be understood, the different dILPs are produced in various cell types and tissues in specific spatiotemporal patterns during development, this suggests that the dILPs have different functional roles in the adult fly (Nässel et al., 2013).While there are eight different dILPs there is only one insulin receptor (dInR). dInR has a high affinity for the dILPs and binds

to all eight of the known dILPs (Nässel et al., 2013). dInR is homologous to human insulin receptor. Unlike in *Drosophila,* humans only have one Insulin Receptor (IR) (Semanik et al., 2018). Once a dILP is bound to dInR the receptor phosphorylates an insulin receptor substrate (IRS) called CHICO. This results in downstream signaling events. After the phosphorylation of CHICO downstream events are achieved by binding of D110 and activation of protein kinase B/AKT. Following B/AKT activation a downstream signaling pathway called Target of rapamycin (TOR) is activated. TOR, a downstream signaling pathway, becomes active to modulate gene expression in response to nutrient intake and serves as a negative regulator of autophagy (Hirabayashi et al., 2013). When insulin signaling is inhibited, TOR signaling is inhibited as well. TOR is found to be involved not only in cell growth regulation but also in carbohydrolyisis, lipolysis and autophagy for example, in the fat body (Teleman, 2010). Phosphorylation of *Drosophila* forkhead transcription factor (dFOXO) is necessary for localization and transcriptional activity, modulating stress response, growth and proliferation (Figure 3). dFOXO activation can occur during times of nutrient restriction, amino acid starvation, and oxidative stress. These all can result in inhibition of growth and development in an individual (Biglou et al., 2021).

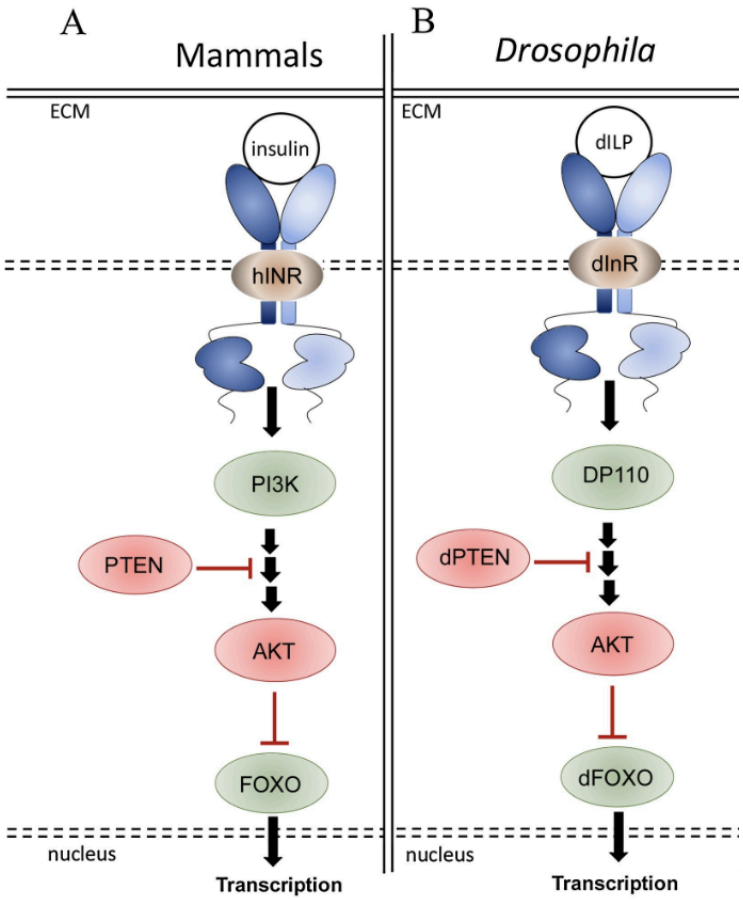

Figure 2. Simplified Diagram Illustrating the Insulin Signaling Pathway Following Receptor Binding in the Extracellular Matrix (ECM). (A) Mammalian insulin pathway: Following binding of insulin with the insulin receptor, downstream signal transduction is initiated. Phosphoinositide 3-kinase (PI3K) is recruited and activated leading to phosphorylation of downstream targets, phosphatase and tensin homolog (PTEN) inhibit the pathway via phosphatase activity. Activation of PI3K leads to activation of downstream component AKT that in turn inhibits the translocation of forkhead box-containing protein, from the O subfamily (FOXO) into the nucleus and transcription of genes occurs. (B) *Drosophila* insulin pathway. DP110 is the *Drosophila* homolog of mammalian PI3K that is activated following binding of *Drosophila* insulin-like peptides (dILPs) to the *Drosophila* insulin receptor (dInR). The pathway is inhibited by *Drosophila* PTEN. Following receptor activation *Drosophila* FOXO (dFOXO) is sequestered and is unable to translocate to the nucleus where it is involved in transcription of genes (Figure from Biglou et al., 2021).

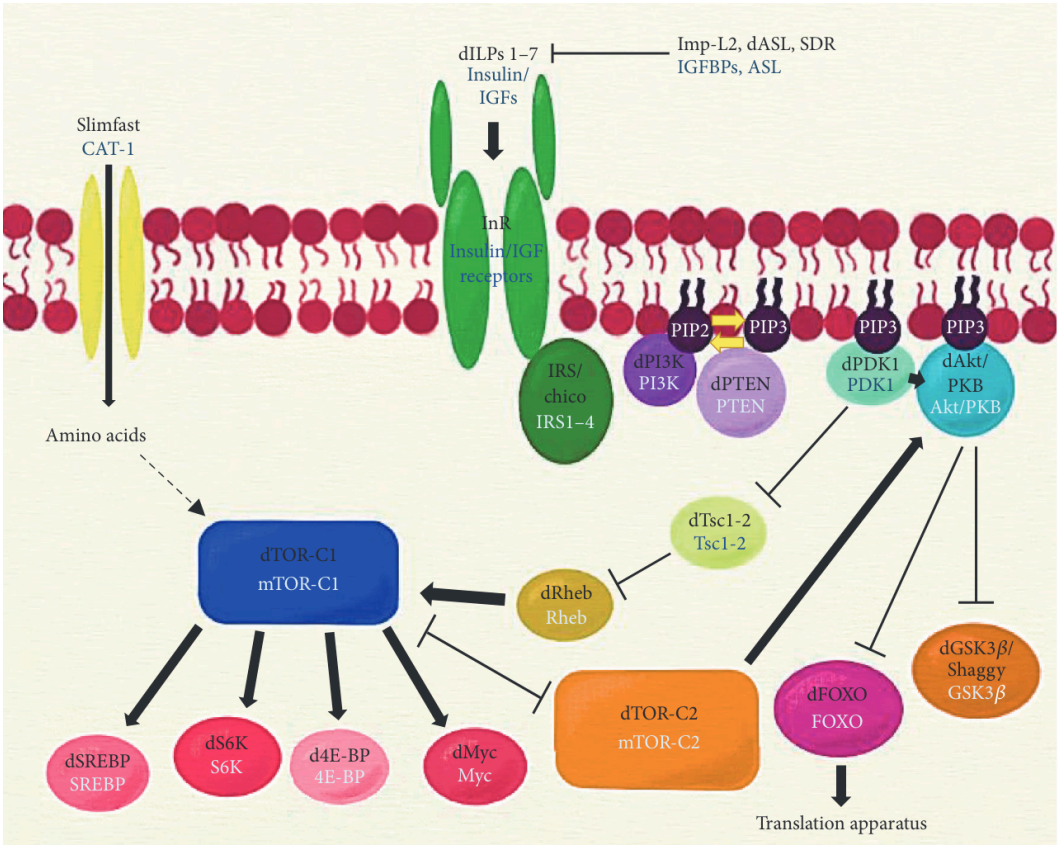

Figure 3. The *Drosophila* Insulin Signaling Pathway: Activation of PlK3 Signaling and TOR Signaling Pathways. Upon dILP ligand binding to dInR PlK3 signaling pathway is turned on. The activation of Chico, PKB and dPDK1 act downstream of dInR to suppress dFOXO and the activation of the TOR pathway. dFOXO gets phosphorylated and can no longer act inside the cell nucleus. Dashed lines represent indirect interaction. Arrows represent activation and bar-headed lines represent inhibition (Figure from Álvarez-Rendón, Salceda, and Riesgo-Escovar, 2018).

Regulation of Insulin signaling by ecdysone

20-hydroxyecdysone (ecdysone), is a steroid hormone produced mainly in the prothoracic gland found in insects including *Drosophila*. Ecdysone is involved in cell proliferation, growth, and apoptosis. Ecdysone plays a crucial role in

regulating physiological processes including molting and metamorphosis (Yamanaka et al., 2013). The structure of the ecdysone hormone is consistent with other hormones containing a three-membered ring attached to a single five-membered ring (Aranda and Pascual, 2001). The solubility of ecdysone allows it to diffuse through the membrane of target cells and bind to its receptor, producing allosteric changes. Ecdysone orchestrates molting, ecdysis, and eclosion events throughout the *Drosophila* life cycle. Ecdysone is necessary and responsible for regulating the transition between different developmental stages and tissue remodeling in the fat body (Bond et al., 2011). It acts through a complex signaling pathway involving nuclear hormone receptors and gene expression, ultimately regulating the intricate changes in morphology and behavior characteristic of insect development (Figure 4).

Ecdysone, in addition to playing a large role in larval development and metamorphosis, is involved in the regulation of insulin signaling. It has been suggested that ecdysone together with insulin signaling regulate growth during larval development (Colombani et al., 2005). It has been previously hypothesized that ecdysone acts as an upstream regulator of the insulin signaling pathway and therefore indirectly blocks the TOR signaling pathway (Bond, 2010; Colombani et al., 2005). Growth in *Drosophila* is facilitated by dILPs. dILPs are released into the hemolymph and bind to dInR. This initiated insulin-like growth factor signaling (IIS) cascade. Reducing IIS by removing insulin-producing cells or key

effectors can result in decreased growth, metabolic dysfunction and is characterized by a diabetic-like phenotype (Buhler et al., 2018). Growth and maturation are coordinated processes that intercommunicate with one another.

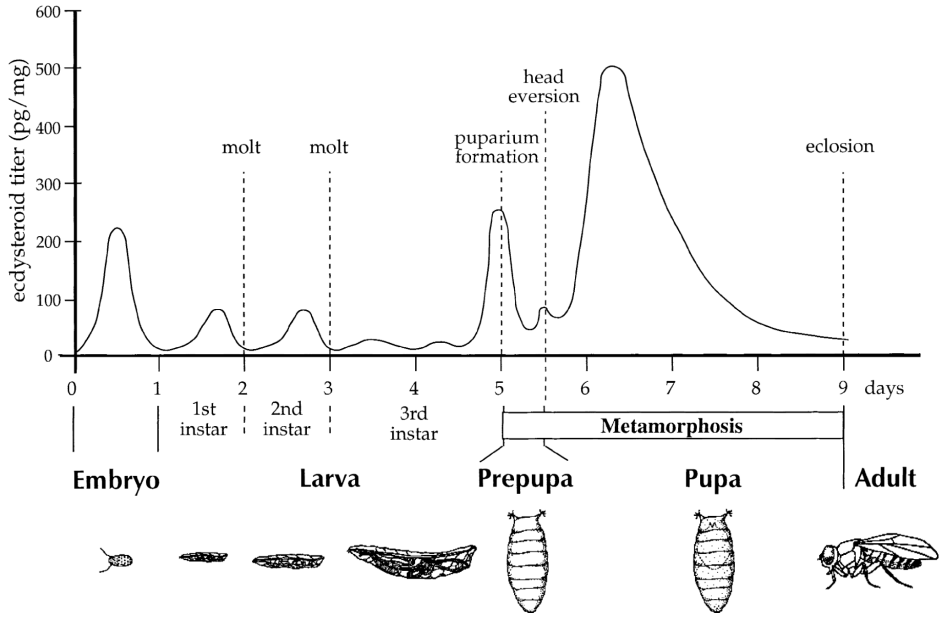

Figure 4. Ecdysone Pulses Trigger Each of the Major Developmental Transitions in *Drosophila*. Major developmental changes are marked by dotted lines. Each post-embryonic transition is marked by an increase in ecdysone titer. A high pulse of ecdysone initiates Puparium formation and head Eversion, at 0 hours after puparium formation (APF) and 10-12 hours APF (Figure from Thummel, 2001).

Insulin Signaling and MMP2

One type of molecule that is hypothesized to play a role in insulin signaling are the matrix-metalloproteinases (MMPs). MMPs are an extensive family of enzymes responsible for the degradation and remodeling of extracellular

matrix (ECM) proteins and are capable of intracellular and extracellular cleavage for various physiological and pathological processes including wound healing, angiogenesis, and cell migration (Gou et al., 2023; Jia et al., 2017). MMPs are tightly regulated endogenous inhibitors called tissue inhibitors of metalloproteinases (TIMPs). TIMPs bind to active MMPs, forming complexes that prevent MMP-mediated ECM degradation. The expression and activity of MMPs are essential for various physiological processes, including tissue repair (Jia et al., 2017). However, dysregulated MMP expression is associated with numerous pathological conditions, such as cancer metastasis, inflammatory diseases, and metabolic dysfunction (Hirabayashi et al., 2013). Therefore, understanding the mechanisms controlling MMP expression and activity is critical for developing therapeutics targeting these enzymes. There are MMPs in insects and mammals. In mammals 24 MMPs have been identified (Cieplak and Strongin, 2017). In *Drosophila* there are two MMPs; MMP1 and MMP2.

In *Drosophila*, there are two proteins that have functional similarities to mammalian insulin-like growth factor-binding proteins (IGF-BPs); *Drosophila* Insulin-like Growth Factor-Binding Protein Acid-Labile Subunit (dALS) and Imaginal morphogenesis protein-Late 2 (Imp-L2). Both dALS and Imp-L2 are involved in insulin signaling in *Drosophila*. Imp-L2 has been identified as the mammalian ortholog of IGFBP-rP1 as it shares many functional and structural similarities with IGFBP-rP1 (Arquier et al., 2008). Imp-L2 has been identified as

the homolog of vertebrate IGF-binding protein 7. It has been suggested that Imp-L2 suppresses insulin signaling as it binds to *Drosophila* insulin-like peptide 2 (dILP-2). It is thought that the Imp-L2-dILP-2 interaction enables dILP-2 to phosphorylate InR. Imp-L2 is an inhibitor of growth and essential for the endurance of periods of starvation. During periods of starvation nutrient release becomes essential for an individual's survival. During this time Imp-L2 expression increases causing glycogen and lipid release. Overexpression of dILP-2 seems to require Imp-L2 to control. This is known as hyperinsulinemia (Honegger et al., 2008).

The mammalian homolog of insulin-like growth factor-binding protein acid-labile subunit (IGF-BP-ALS) is known as dALS (Arquier et al., 2008). In mammals IGF-BP and ALS bind to form various complexes (Biglou et al., 2021). dALS binds to both dILPs and Imp-L2 forming a trimeric complex. If binding between dALS and Imp-L2 does not occur, dALS is unable to bind dILP. When this complex is formed it is involved in growth regulation. dALS regulates growth and metabolism through this trimeric complex by responding to fluctuations in nutrient availability. During periods of starvation, dILPs are found to be limited in numbers. Upon starvation, dALS prolongs the half-life of the dILPs. This interaction provides *Drosophila* with some resistance to starvation. Alternatively, when there is an excess of nutrients, dALS acts as an inhibitor of growth in an individual (Arquier et al., 2008).

MMPs induce the release of growth factors by binding growth factor-binding proteins (IGF-BPs). Various MMPs serve as IGF-BP-cleaving proteins. Alterations in MMP expression may be associated with adverse health outcomes including cancer metastasis and metabolic dysfunction (Cui, Hu, and Khalil, 2017). Cleavage of IGF-BP by MMP7 in mammals is associated with tumors, MMP-7 it is found to be responsible for enhancing cancer cell growth (Papalexi, 2013). In *Drosophila* the mechanism of insulin signaling regulation is not well understood. If mammalian and *Drosophila* IGF-BP and MMPs are not only structurally but also functionally similar then *Drosophila* MMPs may play a pivotal role in insulin signaling regulation. MMP2 is hypothesized to be involved in insulin signaling regulation because of its involvement with fat body dissociation during metamorphosis. When fat body cells get dispersed, nutrient release occurs. This suggests that insulin signaling is downregulated. This leads to the hypothesis that MMP2 acts as an inhibitor to insulin signaling.

Drosophila melanogaster **as a Model Organism**

Drosophila melanogaster, commonly known as the fruit fly, is a widely used model organism for research genetics and developmental biology. They are often used in research of developmental signaling pathways. *Drosophila* are used in research to address human diseases and signaling pathways and molecular functions in normal and diseased cells due to *Drosophila* having 75% similarity to

all human genes implicated in disease have functional homologs in *Drosophila* (Rubin et al., 2000). Therefore *Drosophila* makes a good model organism to study insulin signaling seeing that it is analogous to mammalian insulin signaling like that of humans. The *Drosophila* fat body is functionally analogous to mammalian hepatic and adipose tissue which are highly susceptible to insulin insensitivity (Jia et al., 2017). *Drosophila* are used as a model for numerous characteristics: they have a rapid life cycle, are small and easily cultured, have an extensively mapped genomen, and male and female individuals are easily distinguishable.

The *Drosophila* Life Cycle

Drosophila undergoes five distinct stages of development; embryonic, larval, prepupal, pupal, and adult (Figure 5). The life cycle starts with fertilization of the egg, after the embryo develops for one day it undergoes the process of embryogenesis and the larva hatches. This is the larval stage. Over the next 8 days the larva undergoes many developmental changes. There are the three distinct larval stages: first, second, and third instar. The transition from one stage to the next occurs through a molting process where the mouth hooks, spiracles, and other essential structures are torn apart and reformed (Demerec, 1950; Notarangelo, 2014). The three larval stages are distinguishable by morphological differences. 1st instar larvae have small mouth hooks. After the first molt, this is

the transition between 1st and 2nd instar, larvae develop larger mouth hooks as well as forming both anterior and posterior spiracles. Posterior spiracles have an orange hue. The second molt occurs, this results in the formation of the 3rd instar. The orange hue in the posterior spiracles continues to darken and the anterior spiracles become shell shaped. During each molt the larvae grow in size. The 3rd instar is divided into two stages, the feeding stage and the wandering stage. Feeding thirds are located in the food and are actively consuming food to hit critical mass. Wandering thirds have crawled out of the fly food in preparation for metamorphosis (Chung et al., 2009). The transition from wandering third to the prepupal stage is followed by formation of the puparium. This marks the beginning of metamorphosis. Puparium formation is used as a marker of time throughout *Drosophila* development, it is denoted as hours after puparium formation (APF). Puparium formation occurs at 0 h APF. During puparium formation the larval cuticle transitions from white to a dark brown color. The individual undergoes tissue remodeling and programmed cell death during the prepupa and pupa stages. Remodeling of the larval fat body occurs, the process by which sheets of attached cells are transformed into single cells into free-floating spherical cells. Head and wing eversion occur. Once metamorphosis is completed the adult fly ecloses (Bond et al., 2011).

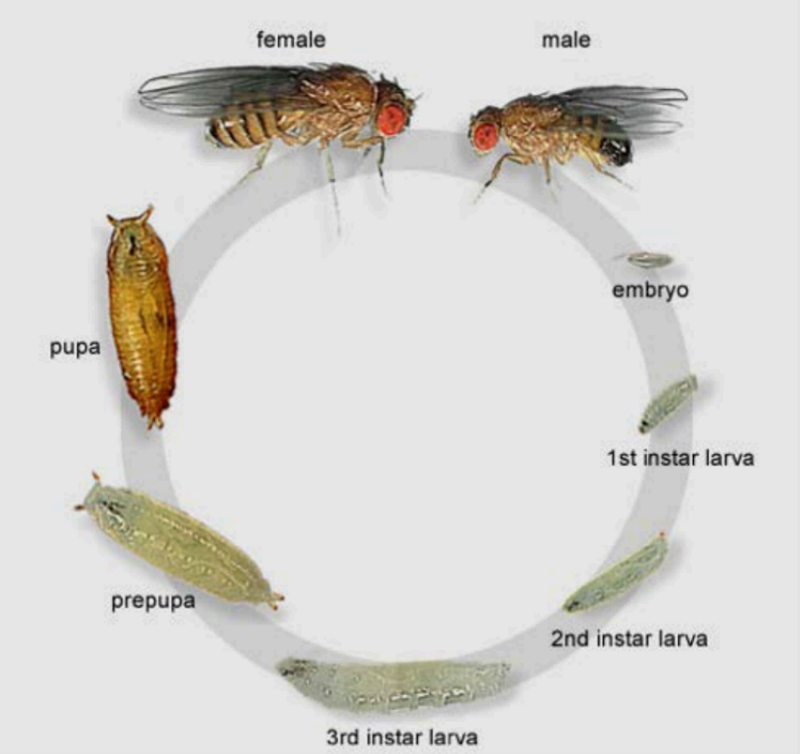

Figure 5. *Drosophila melanogaster* Life Cycle. The stages of *Drosophila* development from embryo to adult. Through molting the larvae develop larger mouth hooks and spiracles. The end of the larval stage is marked by the development of puparium and transformation into a prepupa. This transition marks the beginning of metamorphosis. (Figure from Weigmann et al., 2003)

Metamorphosis

As the *Drosophila* life cycle takes place a process called metamorphosis occurs. During *Drosophila* metamorphosis the individual transitions from a larva, which eats continuously, through a pupal stage in which the individual is undergoing a mandatory 5 day starvation. Ending metamorphosis as an adult fly.

The individual has to survive on nutrient molecules stored in the cells of the larval fat body. During metamorphosis the fat body goes through major changes. The cells transition from energy storage cells to energy release cells and the tissue remodels, breaking up from a sheet of connected cells to individual cells. We have determined some of the key molecular genetic steps that lead to the remodeling of the fat body and the dissociation of the cells from one another.

Metamorphosis is the transition from larva to adult fly. As metamorphosis occurs there are changes in gene expression which lead to transformations in formation of tissue and organs and well as tissue remodeling and destruction. The competency factor βFTZ-F1 plays an important role in tissue changes during metamorphosis. βFTZ-F1 has been shown to be involved in tissue remodeling in the fat body of *Drosophila* (Bond et al., 2011). During metamorphosis individuals undergo a period of starvation in which they must rely on nutrients from the larval fat body (Jia et al., 2017). MMP2 is an enzyme that, during metamorphosis, when the pupa is undergoing starvation, cleaves extracellular matrix proteins and cell-cell junction proteins to allow dissociation of the fat body cells from each other during tissue remodeling (Anding & Baehrecke, 2015; Bond et al., 2011; Notarangelo, 2014).

Fat body Remodeling

Remodeling of the fat body occurs in response to various physiological cues, such as nutrient availability, developmental stage, and environmental conditions. The fat body of *Drosophila* is analogous to vertebrate liver and adipose tissue. The larval fat body is a single-cell sheet consisting of only one cell type. During the prepupal–pupal transition, around 6 hours APF, the larval fat body detaches from a single sheet and becomes spherical. Around 12 hours APF, detachment is complete and fat body cells are fully dissociated into single cells (Figure 6) (Jia et al., 2017). Notably both MMP1 and MMP2 are required to induce fat body cell dissociation. MMP1 cleaves epithelial- cadherin–mediated cell– cell junctions and MMP2 degrades basement membrane components. This leads to the destruction of cell–BM junctions, which leads to dissociation of the fat body into individual cells (Jia et al., 2017). In addition to storing energy, the fat body also plays a central role in regulating systemic growth in response to nutrition. Upon sensing dietary amino acids the fat body secretes several humoral factors, which control systemic growth of the individual. This is due in part to the regulated secretion of dILPs by the insulin-producing cells of the brain. The fat body also plays a role in systemic immunity by expression and secretion of several antimicrobial peptides. Fat body cells are motile which allows them to

migrate to wound sites and undertake local functions to drive wound repair and prevention of infection (Franz et al., 2018).

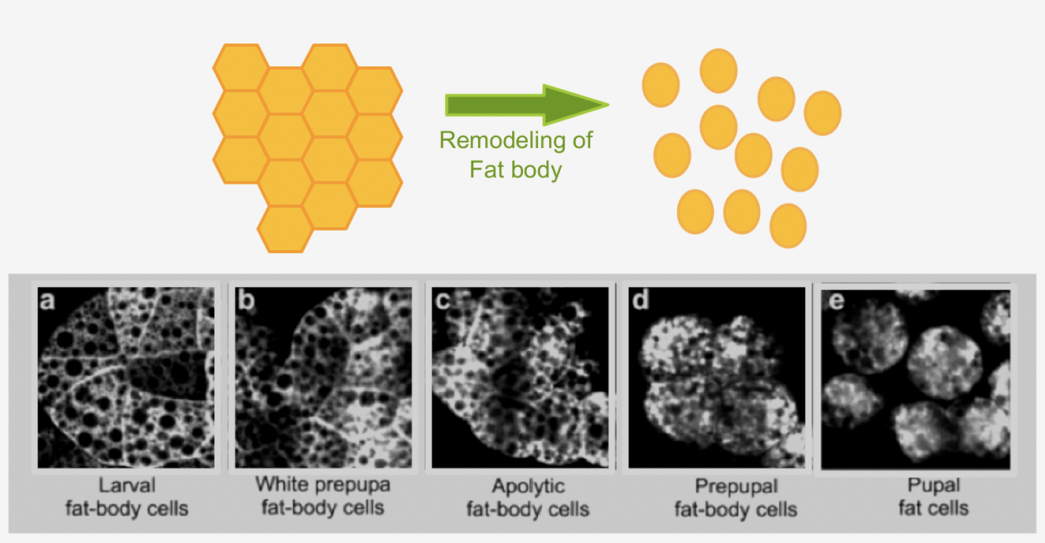

Figure 6. Remodeling of the Larval Fat Body in *Drosophila*. Through metamorphosis the fat body remodels from a single-cell sheet consisting of only one cell type. Around 6 hours APF the larval fat body detaches from a single sheet and becomes spherical. Around 12 hours APF, detachment is complete and fat body cells are fully dissociated into single cells which are motile.

MMPs

Matrix-Metalloproteinases are membrane bound proteases that are part of a family of Zinc dependent membrane endopeptidases (Guo et al., 2023). There are two matrix-metalloproteinases (MMPs) in *Drosophila melanogaster*: MMP1 and MMP2. In mammals there are 24 MMPs. Some MMPs are attached to the cell membrane by glycosylphosphatidylinositol (GPI) which is a membrane anchoring glycolipid allowing some MMPs to be peripheral proteins having a larger

presence near the ECM in the extracellular region (Page-McCaw, 2008). MMPs are membrane bound proteases responsible for breaking down ECM proteins such as laminin, collagen, and fibronectin. When cleavage of ECM proteins occurs, cells lose their attachments. MMPs are expressed in small amounts during standard conditions, affecting the ECM. When MMP2 is uninhibited in the cell they have high rates of degradation of the ECM. This can cause catastrophic cleavage of ECM structures, growth factors, cytokines, and signaling receptors. Therefore, MMPs are regulated by tissue inhibitors of matrix metalloproteinases (TIMPs) (Jia et al., 2017). In mammals there are 4 TIMPs: TIMP-1, TIMP-2, TIMP-3, and TIMP-4 (Brew and Nagase, 2010). Unlike mammals, there is only one TIMP in *Drosophila*. To ensure homeostasis, a balance must be achieved between MMPs and TIMPs (Figure 7). During developmental changes, such as metamorphosis and fat body remodeling the ratio changes and levels of MMP2 increase in *Drosophila* due to an increase in expression of ecdysone which also triggers the increased expression of βFTZ-F1 (Figure 8) (Bond et al., 2011). Opposingly, misregulation of TIMPs leads to failure in fat body remodeling which leads to premature death (Jia et al., 2017). Both MMPs in *Drosophila* cooperatively and individually to ECM structures. MMP1 is responsible for tracheal development and head eversion. MMP2 is responsible for fat body remodeling and is proposed to cleave insulin receptor (Bond et al., 2011; Papalexi, 2013). *MMP2* expression in the larval fat body is regulated by βFTZ-F1

(Jia et al., 2017). It has been previously established that βFTZ-F1 in conjunction with the prepupal pulse of ecdysone induce *MMP2* expression. Bond and colleagues in 2011 observed that ectopic βFTZ-F1 expression led to premature *MMP2* expression (Bond et al., 2011). Overexpression of *MMP2* in the larval stage causes fat body cells to separate from a single layered sheet to individual spherical cells (Bond et al., 2011; Jia et al., 2017). MMP1 has roles in early cleavage but is not sufficient for fat body remodeling. On the other hand, MMP2 is both necessary and sufficient for induction of fat body remodeling (Bond et al., 2011). MMP2 is important in fat body remodeling and has the potential to cleave insulin receptor (InR).

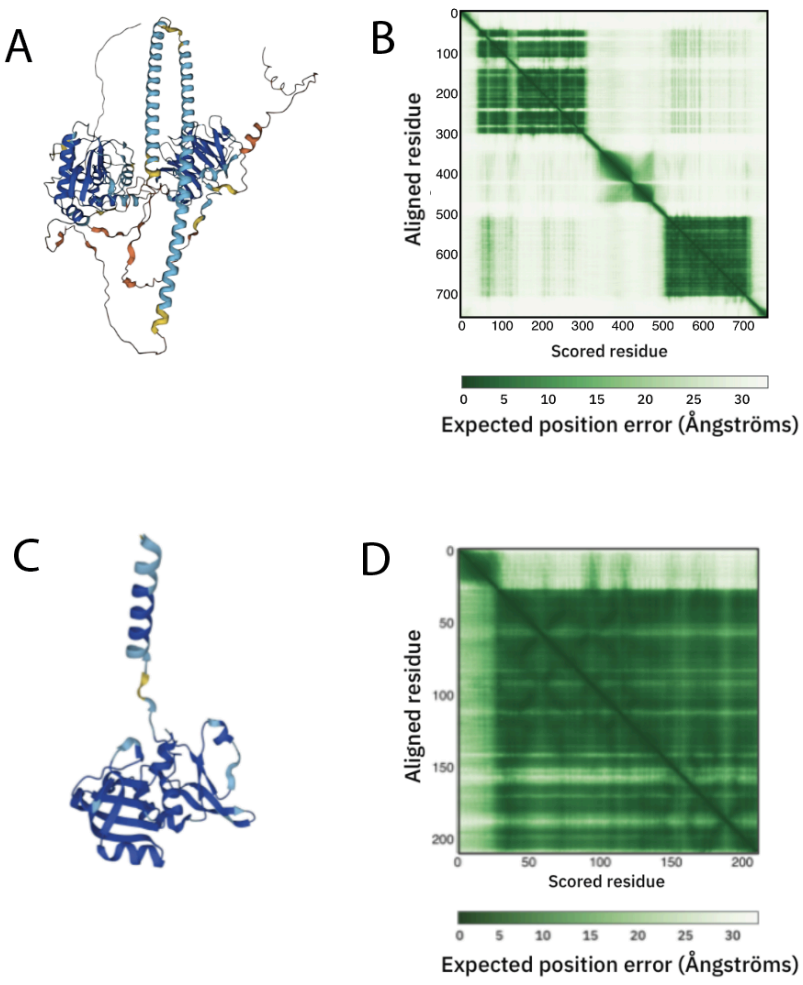

Figure 7. Predicted Structures Matrix Metalloproteinase-2 and Tissue Inhibitors of Matrix Metalloproteinases in *Drosophila melanogaster*. Neither Matrix Metalloproteinase-2 (MMP2) or Tissue Inhibitors of Matrix Metalloproteinase (TIMP) have a confirmed crystal structure. Therefore we are reliant on predicted structures from software. Theoretical model from AlphaFold protein structure database. (A) Predicted protein structure of MMP2. (B) Predicted Aligned Error (PAE) of MMP2. PAE measures the confidence in the relative position of two residues within the predicted structure. PAE provides insight to the reliability of relative position and orientation of specific domains. (C) Predicted structure of TIMP. (D) PAE for TIMP.

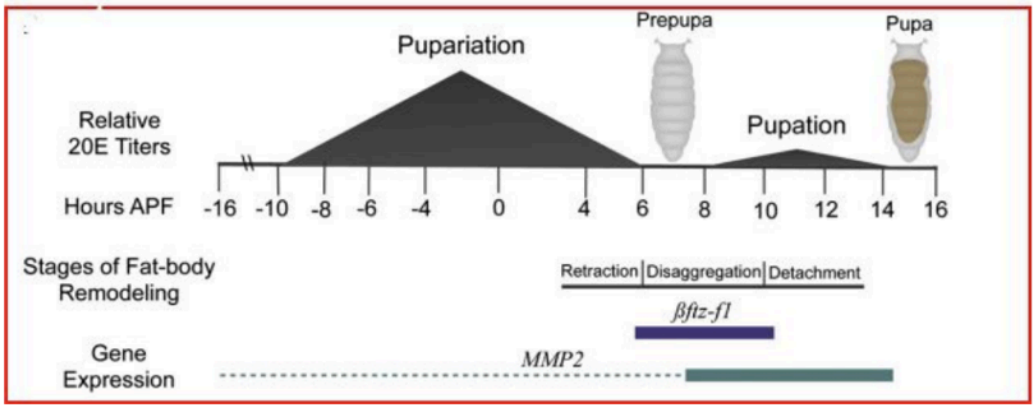

Figure 8. 20-hydroxyecdysone Signaling and βFTZ-F1 Involvement in Induction of Matrix Metalloproteinase 2 Expression in the Larval Fat Body. Relative expression levels of *MMP2* in dissected fat bodies from different time points. At 6 hours after puparium formation (APF) low titer of ecdysone causes the transcription of *βFTZ-F1*. This induced the transcription of *MMP2* around 10 hours APF. Once *MMP2* is transcribed it cleaves ECM proteins, disconnecting the attachments between fat body cells. Fat body cells go from one contiguous sheet to free floating individual cells in the larva (Figure from Bond, 2011).

In mammals the 24 MMPs play roles in many different processes, including extracellular matrix cleavage, bone, and cartilage remodeling, cancer mastitis, cell proliferation, wound healing, age associated insulin resistance and angiogenesis (Papalexi, 2013; Guo et al., 2023). Serval MMPs have been shown to cleave IGF-BPs. The characteristics of mammalian MMPs facilitate the release of IGF which regulates growth. In mammals MMPs have been shown to enhance cancer cell growth. In *Drosophila* the mechanisms for insulin regulation is not entirely known. *Drosophila* and mammalian IGF-BP are structurally similar, hence *Drosophila* MMP2 might play a pivotal role in the regulation of insulin

signaling (Papalexi, 2013). MMP2 is involved in fat body remodeling during metamorphosis (Jia et at., 2017). When fat body cells are dissociated and dispersed throughout the larva, nutrient release occurs; this suggests that downregulation of insulin signaling occurs (Bond, 2010). This led to the line of thinking that MMP2 is directly acting on insulin signaling as an inhibitor. In 2010 Nichole Bond proposed a model in which IGF-BP (Imp-L2 and dALS) are cleaved by MMP2. As a result dILPs are degraded and insulin signaling is shut off. In this model nutrient release also occurs to satisfy the energy needs of the individual (2010). The model I proposed is altered from Bond's. In this model MMP2 cleaves insulin receptors shutting off insulin signaling. Insulin sensitivity declines progressively as aging occurs in mammals (Guo et al., 2023).

In a murine model matrix metalloproteinase14 (MMP14) also called MT1/MMP is the mouse homolog for MMP2 in *Drosophila*. MMP14 is a membrane bound zinc containing protease. MMP14 cleaves a wide range of substrates including ECM and growth factor receptors. Mice with defects in MMP14 can exhibit various age associated phenotypes and succumb. These phenotypes include hypoglycemia, a condition that is associated with a reduction in blood glucose which is often associated with type 2 diabetes and obesity in humans (Giugliano, 2008; Guo et al., 2023). In a study Guo et al. found that MMP14 is a central regulator of insulin sensitivity during aging. MMP14 activation in insulin sensitive tissues is promoted during aging. This leads to the cleavage of insulin

receptor by MMP14, and suppresses insulin signaling. MMP14 has shown to directly cleave insulin receptor in the liver of young mice leading to the suppression of insulin signaling. Guo's team also found that inhibition of MMP14 restores insulin receptor expression (2023). Due to MMP2 ability to cleave signaling receptors and involvement of the degradation and remodeling of ECM leads to questions about whether MMP2 in *Drosophila* may also be able to cleave insulin receptor in an overexpressed condition. If MMP2 proves to be a regulator of insulin receptor it may be a promising target for therapeutics for diseases related to insulin sensitivity and metabolic dysfunction (Guo et al., 2023).

Hypothesis

By understanding the mechanisms involved in *Drosophila* insulin signaling regulation we hope to gain a greater understanding of human diseases such as type 2 diabetes, high blood pressure, insulin insensitivity, other metabolic dysfunction, and other age associated pathologies (Hirabayashi et al., 2013; Guo et al., 2023). *Drosophila melanogaster* is a model organism that can be used for finding therapeutic strategies for these diseases, including those that can modulate MMP2 activity in order to help regulate insulin insensitivity.

In my attempt to understand the role of MMP2 in insulin signaling experiments were performed to demonstrate the role of insulin signaling during larval development. I hypothesize that starvation induces *MMP2* expression to allow MMP2 to cleave insulin receptor, which in turn shuts off insulin signaling, allowing autophagy and nutrient release to occur (Figure 9). In order to test this hypothesis I will examine *MMP2* transcript levels in the fat bodies of fed and starved third instar larvae using real time quantitative PCR. If my hypothesis is correct, I expect to see higher *MMP2* transcript levels in starved samples compared to fed controls.

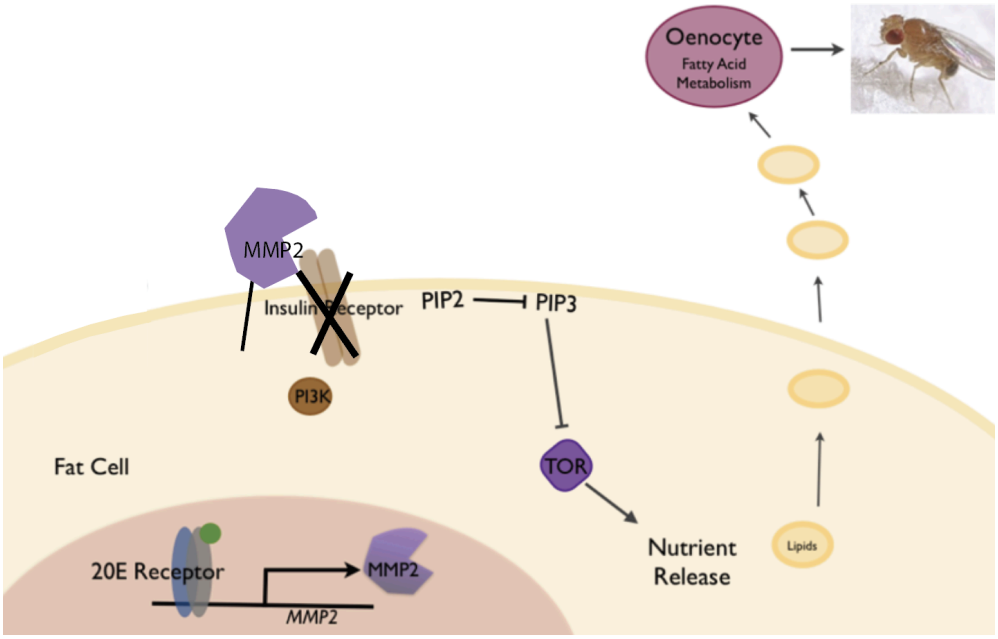

Figure 9. The Proposed Role of MMP2 in Insulin Receptor During Metamorphosis. The ecdysone receptor initiates the transcription of MMP2. MMP2 cleaves insulin receptor. This blocks insulin signaling and consequently represses TOR allowing for nutrient release from the fat body. Lipids are taken from the fat body to the oenocytes and fatty acid metabolism and further development to occur (Adapted from Bond, 2010).

MATERIALS AND METHODS

Fly Stock and Maintenance

The *Drosophila melanogaster* Canton-S (CS) wild type fly stock was raised on Genesee Nutri-Fly® Bloomington Formulation fly culture medium at 25℃ and 50% humidity. *Drosophila* were raised in bottles and transferred to new bottles weekly to maintain a healthy fly stock.

Staging Feeding Third Instar Larvae

Feeding third instars were collected directly from food in the culture bottles and staged by morphology.

Starvation Protocol

Experimental group (STARVED): 15% sucrose was used to separate feeding third instar larvae from food. 10-15 larvae were washed with distilled water and left for 3-4 hours in 20% sucrose prior to dissection (Papalexi, 2013).

Control group (FED): 3-4 hours after separation of the experimental group, 15% sucrose was used to separate feeding third instar larvae from food.

10-15 larvae were washed with distilled water and fat-bodies were immediately dissected from 4-5 larvae. Dissection time for both groups is restricted.

15% sucrose was made by gradually adding 150g of sucrose to 750 mL of distilled water. While the solution was being combined it was placed on a hot plate and a stir bar was added. After the sucrose had gone into solution an additional

250 mL of distilled water was added. The solution was taken off the heat and put through Nalgene™ Rapid-Flow™ Sterile Disposable Filter Units with PES, CN, SFCA or Nylon Membranes. It was imperative to ensure that the solution was sterile. The process was repeated for the 20% sucrose solution with 200g of sugar.

Larval Fat-Body Dissection and RNA Isolation

RNA was isolated from the fat bodies of feeding third instar larvae. The fat-bodies of 4 -5 larvae were collected through dissection and placed in aqueous buffer in separate tubes. For homogenization, TRIzol reagent was added and the sample was ground. After a series of 12,000 rpm centrifugation was completed and chloroform was added the TRIzol pellet was dissolved into RNase-free water. Isopropanol was added and the sample was vortexed and precipitated overnight at

-20℃. The next day the sample was centrifuged at 14,000 rpm for 30 minutes at 4℃, the pellet was just barely visible, the supernatant was removed using a pipet. The remaining pellet was washed with 75% ethanol making it visible and centrifuged at 14,000 rpm for another 10 minutes. The supernatant was removed and the sample tube was then centrifuged briefly using the picofuge, and the residual ethanol was removed from the sample. The pellet was left to air dry for 2 minutes after which RNase-free water was added to redissolve the pellet. The sample was then left at room temperature for 5 minutes before being stored at -20℃ (Table 1).

Table 1. Reagents for RNA Isolation

Component	**Amount per Reaction (µL)**
Aqueous Buffer	30.0
TRIzol	300.0
Chloroform	60.0
RNase-free water	200.0
Isopropanol	160.0
75% ethanol	500.0
RNase-free water	5.0

cDNA synthesis using Oligo(dT)

Each component was centrifuged briefly before being used. To make the master mix, all of the components were combined together in a sterile 0.5 mL tube. The master mix included everything except for the RNA (Table 2).

Table 2. Reagents for Master Mix 1

Component	**Amount per Reaction (µL)**
RNA	1.0
10 mM dNTP mix	1.0
Primer (0.5 µg/µL oligo (dt))	1.0
DEPC-treated water	7.0

The RNA primer was incubated for 5 minutes at 65℃ and was then placed on ice for one minute. In another tube master mix 2 was prepared by combining all of the components (Table 3).

Table 3. Reagents for Master Mix 2

Component	**Amount per Reaction (µL)**
10X RT buffer	2.0
25mM $MgCl_2$	4.0
0.1 M DTT	2.0
RNaseOUT (40 U/µL)	1.0

9 µL of master mix 1 were added to each RNA primer mixture and centrifuged shortly to mix. The sample was incubated at 42℃ for 2 minutes and then 1 µl of SuperScript™ II RT was added. For the Minus RT control 1 µL DEPC-treated water was added instead. The sample was incubated at 42°C for 50 minutes. The reaction was terminated at 70°C for 15 minutes and then chilled on ice. The sample was centrifuged and collected by adding RNase H to the sample and incubating it for 20 minutes at 37°C. The sample was then stored at -20°C to be used for PCR.

RNA Quantification

The concentration of RNA samples was measured using the nanodrop spectrophotometer, TheremoFisher Scientific ND-1000 spectrophotometer (Figure 10).

#	Sample ID	User name	Date and Time	Nucleic Acid Conc.	Unit	A260	A280	260/280	260/230	Sample Type	Factor
1	Fed 1	ke106instr	4/2/2023 4:39 PM	541.9	ng/µl	13.549	6.817	1.99	1.86	RNA	40.00
2	Fed 2	ke106instr	4/2/2023 4:42 PM	255.5	ng/µl	6.388	3.774	1.69	0.38	RNA	40.00
3	Fed 3	ke106instr	4/2/2023 4:49 PM	211.3	ng/µl	5.283	2.695	1.96	1.05	RNA	40.00
4	Starved 1	ke106instr	4/2/2023 4:50 PM	339.3	ng/µl	8.482	4.552	1.86	0.71	RNA	40.00
5	Starved 2	ke106instr	4/2/2023 4:52 PM	206.7	ng/µl	5.168	2.994	1.73	0.44	RNA	40.00
6	Starved 3	ke106instr	4/2/2023 4:53 PM	222.2	ng/µl	5.555	2.976	1.87	0.60	RNA	40.00

Figure 10. RNA Concentrations. Image of the RNA concentrations for control (fed) and experimental (starved) samples. The minimum nucleic acid concentration to be used in the study was 200 ng/ µL and the 260/280 had to be greater than 1.5.

Reverse Transcriptase Polymerase Chain Reaction (PCR) and Gel Electrophoresis

PCR was performed in order to detect cDNA corresponding to *MMP2* transcripts in feeding third instar larvae. Gene specific primers were used to perform this technique. Previously designed *MMP2* and *Actin 5C* forward and reverse primers were used. Primer sequences were obtained from Efi Papalexi (2013) and shown in Table 4. PCR was prepared with First Strand SuperScript® Reverse Transcriptase System kit for RT-PCR (Table 5), it was run on a thermocycler by Techgene (Table 6). cDNA was amplified using RT-PCR.

Table 4. *MMP2* and *Actin 5C* Primer Sequences

Primer	**Sequence**
MMP2 forward	5'-AGCAATCCGGAGTCTCCAGTCTTT-3'
MMP2 reverse	5'-TGGAGCCGATTTCGTGATACAGGT-3'
Actin 5C forward	5'- TCTACGAGGGTTATGCCCTT-3'
Actin 5C reverse	5'-GCACAGCTTCTCCTTGATGT-3'

Table 5. Master Mix for RT-PCR

Reagent	**Amount per reaction (µL)**
10X PCR Buffer (minus $MgCl_2$)	5.0
25 mM $MgCl_2$	6.0
10mM dNTPs	1.0
10 µM forward Primer	2.0
10 µM reverse Primer	2.0
cDNA	2.0
Nuclease-free water	31.0
Taq Polymerase 0.4 µL	0.4

Table 6. Thermocycler Profile for RT-PCR

Stage	**Temperature (°C)**	**Duration/cycle count**
Denaturation	94	30 seconds / 35 cycles
Annealing	58.2	30 seconds / 35 cycles
Extension	72	30 seconds / 35 cycles
Final extension	72	5 minutes /1 cycle
Final hold	4	Indefinitely

Both *Actin 5C* and *MMP2* were put in the thermocycler at the same time because of the similarity in their annealing temperatures. The annealing temperature from

Bond et al. (2011) was used. Gel electrophoresis was then used to visualize the products of PCR.

Real-time quantitative PCR

cDNA shown to be quality was used as a template to assess *Actin 5C* and *MMP2* transcript levels from fed and starved using real time quantitative PCR. The goal of real-time quantitative PCR (RT-qPCR) is amplification and quantification of the target sequence. The target for the primers is *MMP2* and the reference is *Actin 5C* . If the hypothesis is supported insulin signaling will be repressed in the larva due to starvation. *MMP2* will be overexpressed in the starved larvae in comparison to the fed control. RT-qPCR was used to do the relative quantification of the target gene transcript levels in fat body tissue of starved larvae in comparison to the fed control.

As the reaction takes place, RT-qPCR detects the amplification of DNA. The fluorescent dye, SYBR® Green, is used to detect PCR product molecules by binding to dsDNA product and emitting a green fluorescence. This technique was used to quantify levels of *MMP2* and *Actin 5C* transcript in fat body tissue of starved larvae in comparison to the fed control. The reaction was set up on a 96-well plate (Table 12). The master mix utilized for both *MMP2* and *Actin 5C* is shown in Table 7. Each well held 1 µL of cDNA along with 24 µL of the

appropriate master mix. The use of a master mix assured that there was less pipetting, this allowed for the concentrations of the reagents to be consistent between samples along with lowering risk of contamination. Additionally it saved time. The stages of RT-qPCR are shown in Table 8. The qPCR machine used was an Agilent Technologies AriaMx Real-Time PCR System and the software used to view the data was Ailgent AriaMx. The data was analyzed using Pfaffl's equation (Pfaffl, 2001).

Table 7. RT-qPCR Master Mix

Reagent	**Amount per reaction (µL)**
PowerUp ™ SYBR ™ Green Master Mix	12.5
10 µM forward primer	1.0
10 µM reverse primer	1.0
cDNA	1.0
Nuclease-Free Water	9.5

Table 8. Thermocycler profile for RT-qPCR

Stage	**Temperature (°C)**	**Duration/cycle count**
Taq activation	95	2 minutes / 1 cycle
Separation	95	15 seconds / 40 cycles
Annealing	58.2	30 seconds / 40 cycles
Extension	72	30 seconds / 40 cycles
Dissociation		1 cycle

Standard Curve

RT-qPCR required a standard curve to be calculated for the *MMP2* and *Actin 5C* primers. These calculations were used to specify the prime efficiency for each specific amplification experiment. A 10 µL cDNA sample was taken from whole CS larvae to be used as an undiluted cDNA sample. Nuclease free water was used to make 1/2, 1/4, 1/8, and 1/16 dilutions to be used for each standard curve. Each reaction contained 24 µl of the appropriate qPCR master mix and 1 µl of the appropriate cDNA in a single well of a 96-well qPCR plate. At the end of the experiment the qualification cycle (C_q) values from the samples were plotted against the log of the cDNA concentrations and a linear standard curve was obtained. The primer efficiency was calculated using the formula below. Primer efficiencies were thought to be optimal if they were approaching the value of 2.

$$\text{Primer efficiency} = 10^{(-1/\text{standard curve slope})}$$

RT-qPCR Calculations

For each duplicate experimental reaction on the plate the average C_q was calculated. The average C_q values were then used to calculate the ΔC_q(*MMP2*) and the ΔC_q(*Actin 5c*) giving the difference between reference gene, *Actin 5C*, and experimental gene, *MMP2*, expression.

$$\Delta C_q(MMP2) = C_q(MMP2 \text{ fed}) - C_q(MMP2 \text{ starved})$$

$$\Delta C_q(Actin\ 5C) = C_q(Actin\ 5C \text{ fed}) - C_q(Actin\ 5C \text{ starved})$$

The Pfaffl method is then used to calculate the gene expression ratio of fed and starved larvae (Pfaffl, 2001). For this calculation, the reference gene and target gene are essential; the reference gene is *Actin 5C* and the target gene is *MMP2*. The equation proposed by Pfaffl takes into account potentially differing amounts of larval fat body tissue in dissections. The equation also works to correct primer efficiency in order to find the relative expression ratios (Pfaffl, 2001). The ratio is *MMP2* primer efficiency raised to ΔC_q(*MMP2*) all over the primer efficiency of *Actin 5C* raised to ΔC_q(*Actin 5C*). The final calculations indicate the relative expression ratio of the delta C_q values between *MMP2* in starved relative to fed fat body tissue.

$$\text{ratio} = \frac{E(\text{MMP2})^{\triangle \text{Cq(MMP2)}}}{E(\text{Actin5C})^{\triangle \text{Cq(Actin 5C)}}}$$

Statistical Analysis

A two way analysis of variance (ANOVA) was used to decide whether the results obtained from qPCR were statistically significant. Results were considered statistical significance if the p value was less than 0.05.

RESULTS

RNA Isolation

The NanoDrop spectrophotometer was used to analyze the results post-isolation of RNA. This spectrophotometer works by analyzing 1 µl of the RNA sample and it measures the amount of the wavelength of light that has been absorbed by the sample. The 260/280 ratio to be paid attention to while using the spectrophotometer. The 260/280 ratio acts as a detector of any protein contamination. For the sample to be used the number must be greater than 1.5 (Koetsier and Cantor, 2019).

The sample for CS fed third instar larvae fat body had a 260/280 ratio of 1.99, 1.69, and 1.96 respectively. The sample for CS starved third instar larvae fat body had a 260/280 ratio of 1.86, 1.73, and 1.87 respectively. These samples were sufficient to move onto the step of cDNA synthesis.

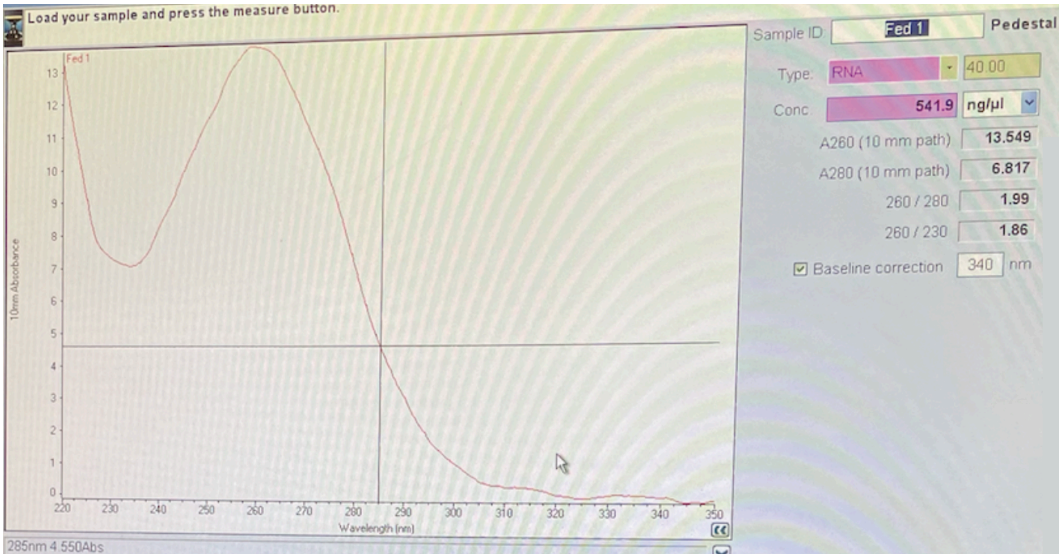

Figure 11. 10mm Absorbance vs Wavelength in nm for CS Fed Third Instar Larvae Fat Body Sample. The 260/280 ratio is 1.99 and the concentration of the nucleic acid is 541.9 ng/µl.

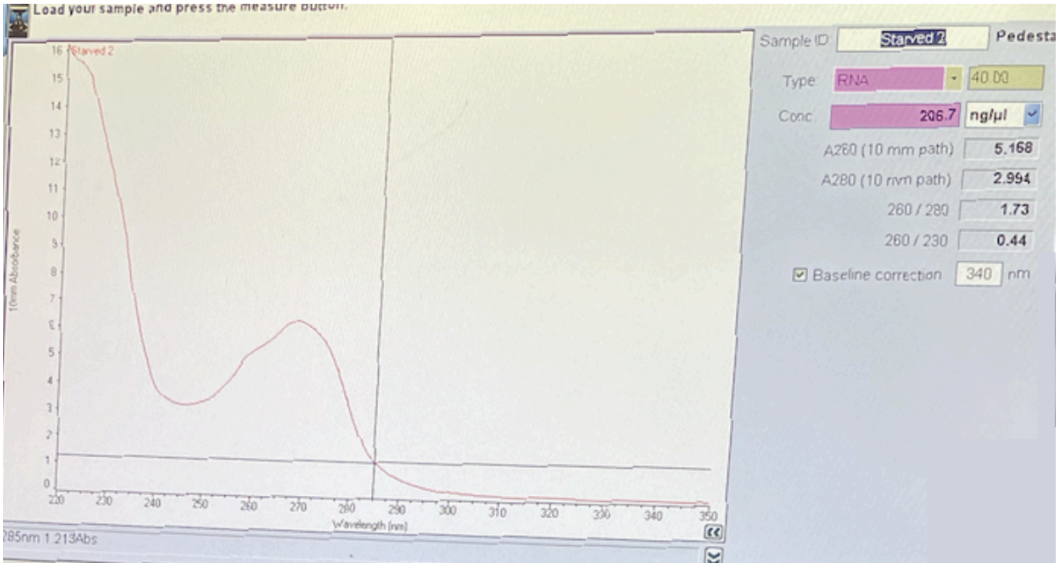

Figure 12. 10mm Absorbance vs Wavelength in nm for CS Starved Third Instar Larvae Fat Body Sample. The 260/280 ratio is 1.73 and the concentration of the nucleic acid is 206.7 ng/µl.

PCR Products and Gel Electrophoresis

Gel electrophoresis was used to visualize the RT-PCR products as well as assessing the primer efficiencies. The samples measured *Actin 5C* and *MMP2* transcript in both fed and starved CS larval fat body isolation (Figure 13 and Figure 14). As seen in figure 13, there is amplification of the target sequence in both *Actin 5C* and *MMP2* starved reactions. *MMP2* and *Actin 5C* starved reactions worked well because of the bands observed in the +RT lanes. On the other hand the Fed reactions for both *MMP2* and *Actin 5C* did not work, indicating that the Fed cDNA was not effective and had to be remade. As seen in figure 14, there is amplification of the target sequence in both *Actin 5C* Fed and Starved. There are bands observed in the +RT lanes of *Actin 5C* Fed and *Actin 5C* Starved. There is no amplification of the target sequence in any of the *MMP2* samples, the reason for which is not completely understood. We are unsure why these *MMP2* primers did not work because they have been used previously in our and published by Bond et al. (2011). Bands of primer dimers were identified in both figure 13 and figure 14. Primer dimer was a byproduct of PCR, possibly because of reduced primer efficiency, The presence of bands in both fed and starved samples show that the samples were successfully converted to cDNA. The combination of these two gel electrophoresis allowed moving forward to RT-qPCT.

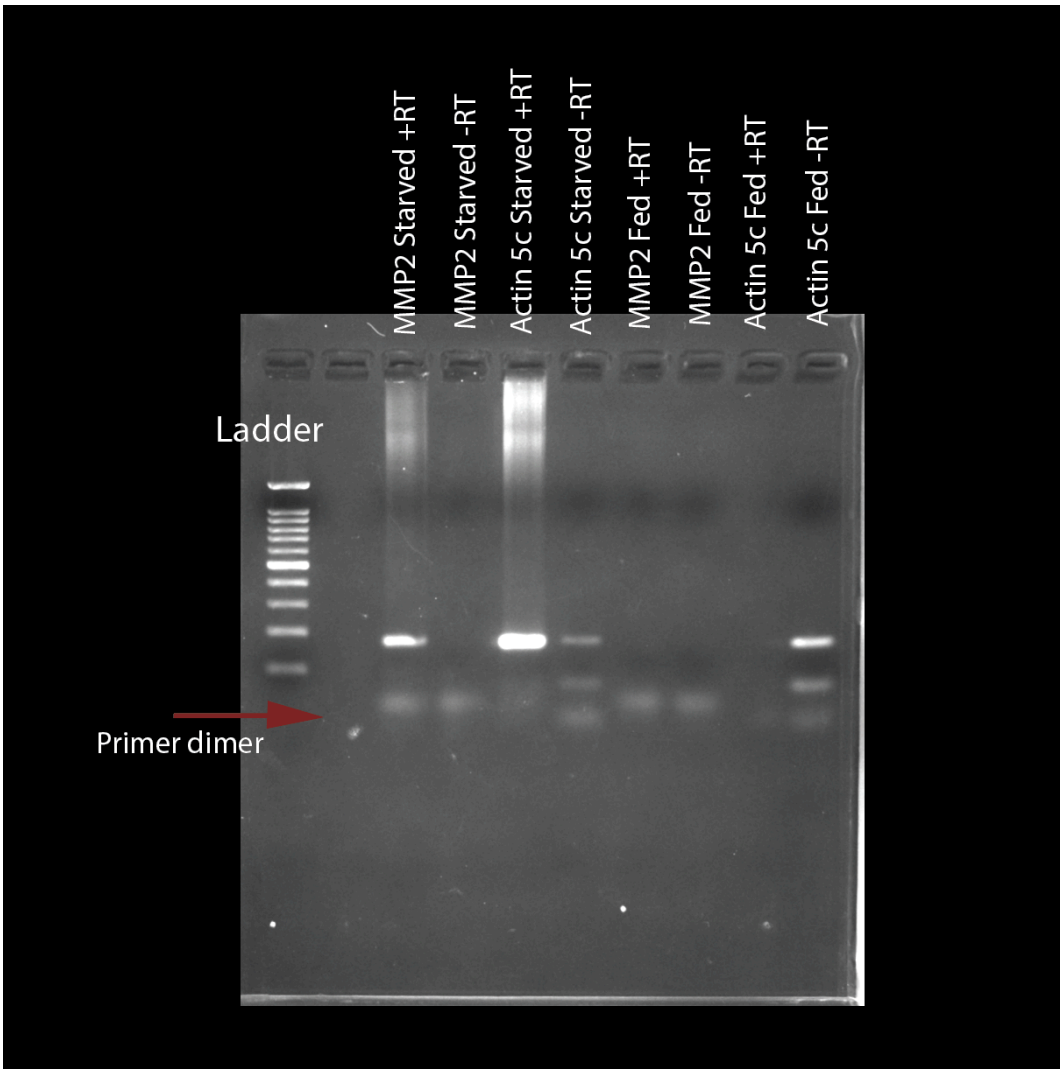

Figure 13. *MMP2*/*Actin 5C* Primer Specific RT-PCR Gel electrophoresis of Fed and Starved Third Instar Larval Fat Body in *Drosophila melanogaster.* Image from February 11 2024. Gel electrophoresis was used to detect the presence of *MMP2* and *Actin 5C* transcripts in both fed and starved larval fat-bodies. A 100 base pair (bp) DNA ladder was added to the first lane and the rest of the lanes are labeled accordingly. There was amplification of *MMP2* starved around 190 bp and amplification if *Actin 5C* starved around 180 bp.

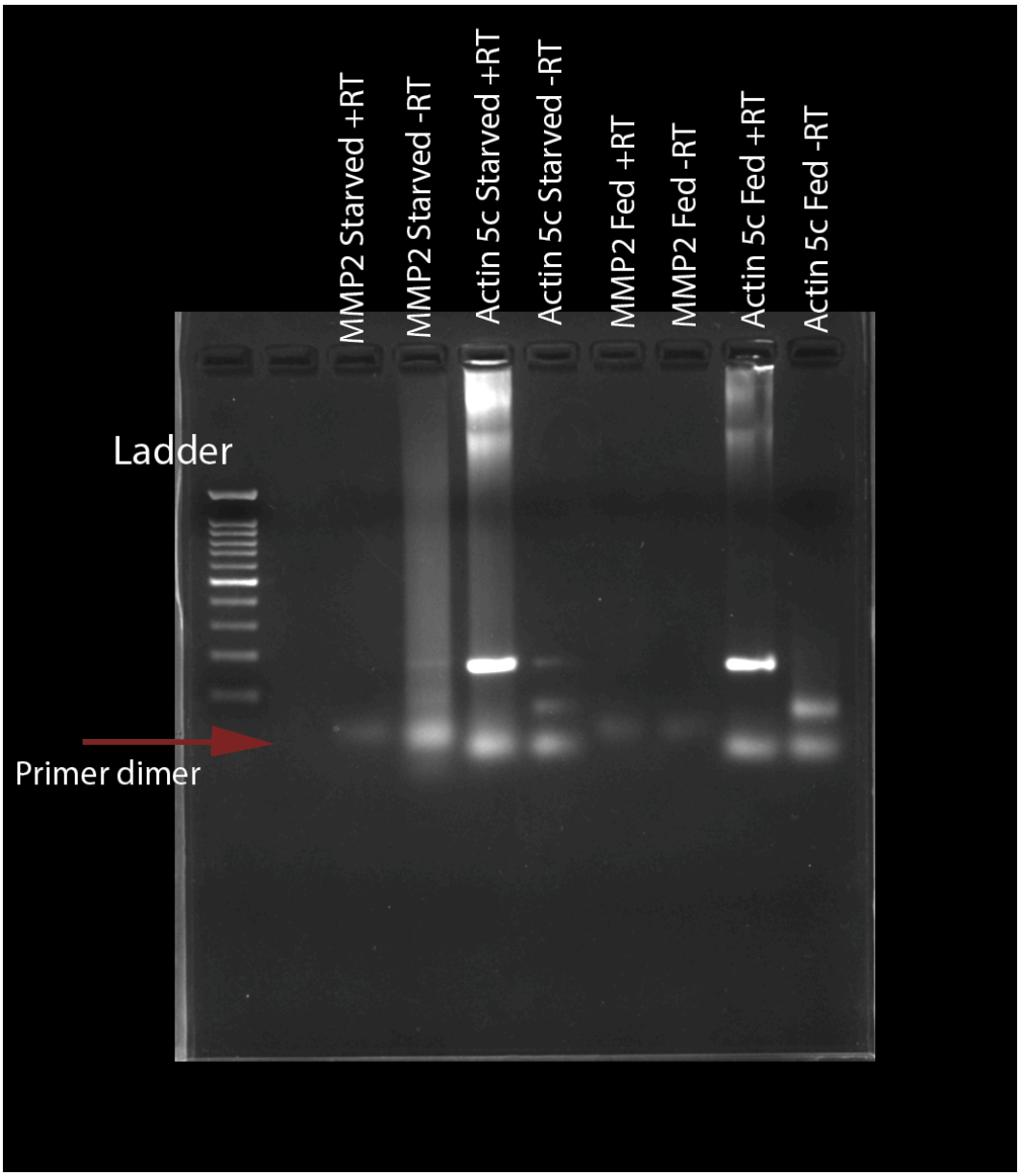

Figure 14. *MMP2*/*Actin 5C* Primer Specific RT-PCR Gel electrophoresis of Fed and Starved Third Instar Larval Fat Body in *Drosophila melanogaster.* Image from February 13 2024. Gel electrophoresis was used to detect the presence of *MMP2* and *Actin 5C* transcripts in both fed and starved larval fat-bodies. A 100 base pair (bp) DNA ladder was added to the first lane and the rest of the lanes are labeled accordingly. There was no amplification of *MMP2*. There was amplification of *Actin 5C* samples around 180 bp.

Quantitative RT-qPCR Standard Curves

Standard curves were set up for every experimental RT-qPCR performed. Each standard curve is specific to the RT-qPCR it was run for. Every experiment had a standard curve for *Actin 5C* and *MMP2*. The standard curves were generated using 5 serial dilutions of CS whole larval cDNA: undiluted, 1/2, 1/4, 1/8, and 1/16. See figures 15-16.

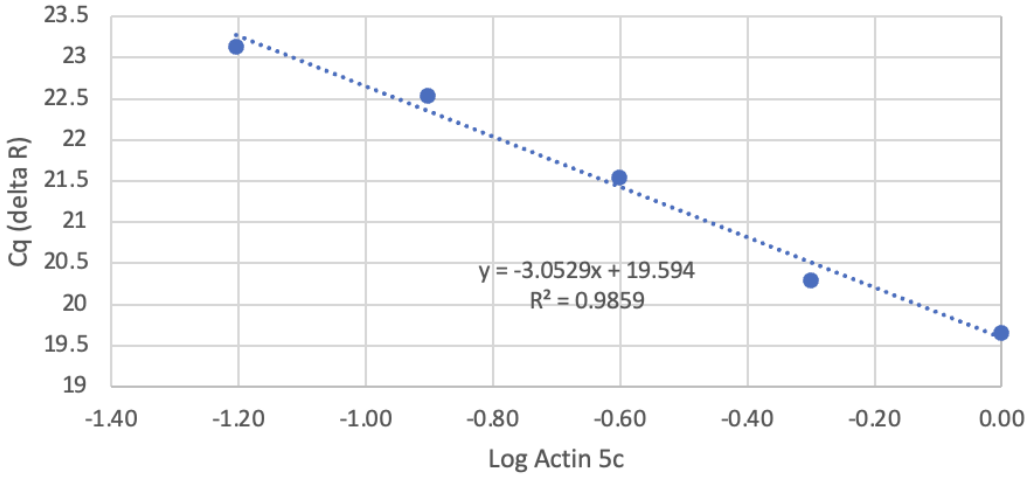

Figure 15. *Actin 5C* Standard Curve. Depicts the log of the concentration of *Actin 5C* dilutions from CS whole larvae plotted against the C_q values. The slope is -3.05 and was used to calculate the *Actin 5C* primer efficiency which was found to be 2.13.

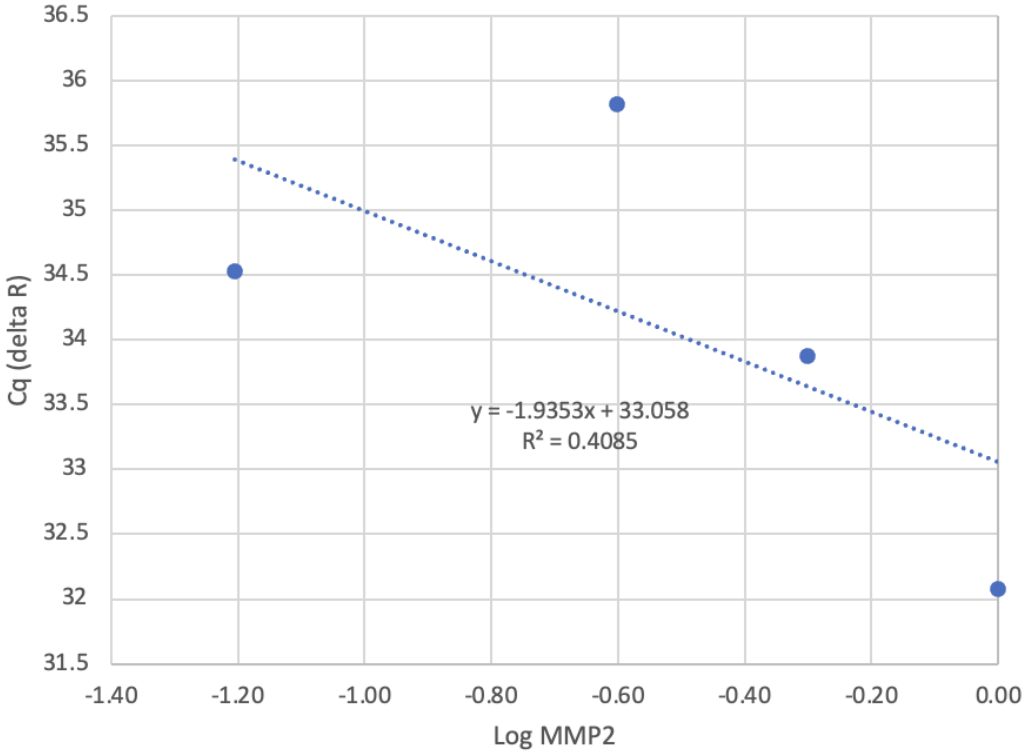

Figure 16. *MMP2* Standard Curve. Depicts the log of the concentration of *MMP2* dilutions from CS whole larvae plotted against the C_q values. The slope is -1.94 and was used to calculate the *MMP2* primer efficiency which was found to be 3.29. Dilutions were excluded due to no C_q value being calculated during RT-qPCR, in this case missing 1/8 dilution.

Table 9. Primer Efficiency Values.

Date	**Primer**	**Efficiency = $10^{(-1/slope)}$**
3/19	*Actin 5C*	2.13
3/19	*MMP2*	3.29
3/23 A	*Actin 5C*	1.93
3/23 A	*MMP2*	2.47
3/23 B	*Actin 5C*	42.37
3/23 B	*MMP2*	3.21

Quantitative RT-qPCR expression ratios

The expression ratios of CS fed larval fat body to starved larval fat body in feeding third instar larvae were calculated using the Pfaffl equation. *MMP2* was used as the gene of interest also known as the target gene. *Actin 5C* was used as the reference gene also known as a housekeeping gene. The hypothesis predicts that *MMP2* will be overexpressed in starved samples in comparison to fed samples. This was supported by each trial's expression ratios along the average expression ratios. According to the Pfaffl equation, 1 is always the expression ratio for the wild-type samples in RT-qPCR (Pfaffl, 2001). Overexpression refers to a ratio greater than 1 and underexpression refers to a ratio less than 1.

Table 10. *MMP2* and *Actin 5C* Expression Ratios. This table shows the expression ratios of fed larval fat body to starved larval fat body in feeding third instar larvae. Overexpression was observed for all dates. Primer efficiency for *MMP2* and *Actin 5C* indicate that they are fit for use.

Date	**Fed/ Starved Expression Ratio**	**Expression in Fed compared to Starved**	***MMP2* primer efficiency**	***Actin 5C* primer efficiency**
3/19/2024	60.1	Overexpressed	3.29	2.13
3/23/2024 A	775.3	Overexpressed	2.47	1.93
3/23/2024 B	16.1	Overexpressed	3.21	42.37

For all three dates the data shows overexpression: all the values are over one. Since the primer efficiency looked reliable was considered for analysis of the results.

Along with a table showing the raw data of *MMP2* and *Actin 5C* expression ratios the results are presented in a chart to better visualize the overexpression of *MMP2* in a starved condition (Figure 17).

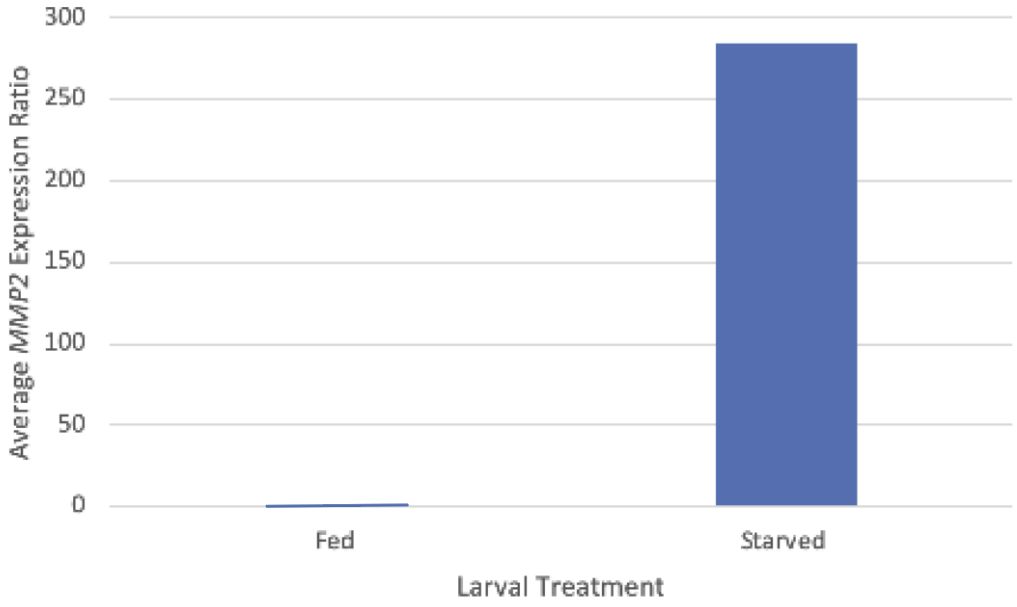

Figure 17. Average Expression Ratio of *MMP2* in Fed and Starved Feeding Third Instar Larval Fat Body of *Drosophila*. The average expression ratios are shown for the RT-qPCR run on 3/19/24, and the two RT-qPCR run on 3/23/24. The fed sample has a constant expression ratio of 1. The average starved expression ratio is 283.8.

Statistical analysis was performed for all data using R studios to determine statistical significance. An ANOVA was performed to determine if there was a significant effect on larval treatment: fed and starved, gene: *Actin 5C* and *MMP2*, and the interaction of larval treatment and gene. Once a significant effect was identified in the model a Tukey test pairwise comparison was performed.

Table 11. Analysis of Variance Data. The table shows the data from the analysis of variance. Larval treatment refers to fed and starved conditions. Gene refers to *Actin 5C* and *MMP2*. Larval treatment: Gene is a comparison of the interaction between the two groups. Statistical analysis was performed to ensure the results were significant (Significance codes $p < 0.01$ *, $p < 0.001$ **, $p < 0$***).

	Degrees of Freedom	**Sum of Squares**	**Mean of Squares**	**F value**	**P value**
Larval treatment	1	22.98	22.98	14.620	0.00506**
Gene	1	291.72	291.72	185.585	8.11e-07***
Larval treatment : Gene	1	15.69	15.69	9.979	0.01342**

After statistical significance was found using the ANOVA (Table 11) a Tukey test was performed to assess the effects of larval treatment on *MMP2*. It was predicted that there would be a difference in the C_q values between fed and starved treatment in *MMP*. This was supported by the Tukey test.

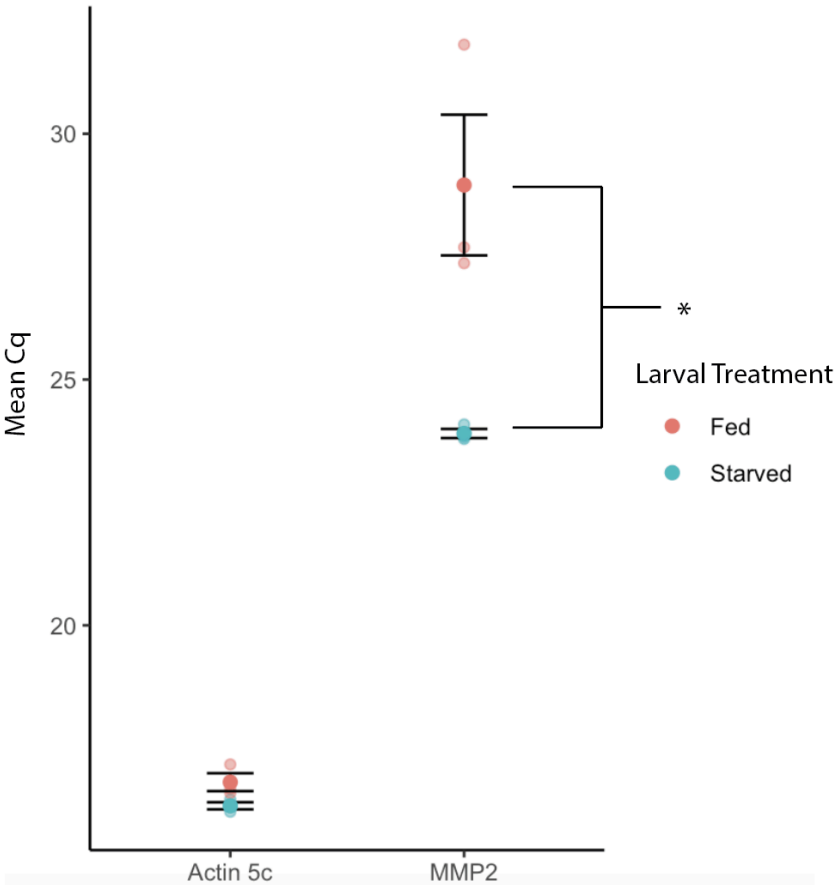

Figure 18. C_q Values for *Actin 5C* and *MMP2* in Fed and Starved Feeding Third Instar Larval Fat Body of *Drosophila*. The mean C_q values are indicated by the darker colored dot. The raw C_q values are indicated by lighter colored dots behind the mean C_q values. The chart shows that there is no significant difference between fed and starved larval treatment in *Actin 5C*. There is a significant difference in C_q values between fed and starved larval treatment in *MMP2*. (Significance codes $p < 0.01$ *)

DISCUSSION

Starvation Experiment and Dissection Observations

Starvation experiments were conducted on CS feeding third instar larvae. During starvation experiments I observed some of the larvae in the starved group start to turn grey. This was an indication of the development of necrotic tissue. These larvae were not used for dissection and RNA isolation. During dissections I observed less fat body tissue in starved samples compared to fed controls.

RNA Isolation Results Observations

Analysis of the fed and starved RNA showed that each sample was satisfactory for use in cDNA synthesis. The nucleic acid concentration for each sample being over 200 ng/ μL and the 260/280 ratio, which indicate the purity of the RNA sample post-isolation, were crucial factors in determining whether to initiate cDNA synthesis. Not all samples used for this investigation had perfect RNA purity, those determined to have a small amount of imperfection were used for cDNA synthesis.

RT-PCR and Gel Electrophoresis Results Observations

The observation and results of RT-PCR and gel electrophoresis had some challenges but ultimately provided helpful insight into determining the next steps of the study. This was because it provided evidence about the efficiency of the primers and the PCR products provided insight on the success of the cDNA synthesis. Challenges included smearing in the lanes of the gel likely due to DNA contamination, amplification of only the reference gene *Actin 5C*, and amplification of only starved samples for both *Actin 5C* and *MMP2*. The 100 bp DNA ladder was used for comparison and analysis. Both the *Actin 5C* and the *MMP2* PCR reactions were successful for starved samples, as shown by bands of PCR product on electrophoretic gels. *Actin 5C* PCR reactions were successful for fed samples, as shown by bands of PCR product on electrophoretic gels. After several attempts there was no band of product in *MMP2* fed samples. The reason for failure to get bands for some samples is unclear because the sample primer and cDNA were used for the other samples that had amplification. Once cDNA was determined to be quality I proceeded to RT-qPCR since it was difficult to draw conclusions from these findings.

RT-qPCR Results Observations

The goal of RT-qPCR was to quantify the data in terms of relative gene expression ratio in order to analyze the amount of DNA present. The results of all three RT-qPCRs indicate overexpression of *MMP2* in a starved condition compared to fed controls in *Drosophila* third instar larval fat body. In conventional PCR there were primer dimers present in the samples. The problem with the primer dimer was resolved during RT-qPCR. Melt curves were normal melting temperatures were around 80℃ indicating that the fluorescence was due to full length PCR products and not primer dimer. The sample size for the data was a total of three runs. Each run showed overexpression but differing amounts. The first run had an expression ratio of 60.1, the second run had an expression ratio of 775.3, and the third run had an expression ratio of 16.1. In order to better compile the results the average of the relative expression ratios were calculated and graphed comparing fed and starved samples. All of the samples were compared using their relative expression ratios of *MMP2*. For fed, this is constant at 1 because the control tissue has a constant expression ratio. The starved samples show varying levels of *MMP2* expression, the average relative expression ratio is 283.8. The expression ratio for all starved samples was over 1 which indicates overexpression. An ANOVA was performed to determine significance and a Tukey test was performed to analyze the effect of larval treatment on

MMP2. As predicted, there was a significant difference between the C_q values of fed and starved larval treatments in *MMP2*. There was no significant difference between the C_q values of fed and starved larval treatments in *Actin 5C* (Figure 18). The primer efficiencies, calculated using the Pfaffl method, are important to note when analyzing the results of RT-qPCR (Pfaffl, 2001). The primer efficiencies for *MMP2* and *Actin 5C* were reasonable, excluding the *Actin 5C* primer efficiency from trial three, allowing for their data to be considered reliable and valid. The reason for the *Actin 5C* primer efficiency from trial three not being valid is unknown, but could be due to sampling error. In some of the primer efficiencies some samples were excluded because they did not provide results during RT-qPCR. These samples were excluded when calculating primer efficiency. Overall, the data suggests overexpression of *MMP2* in the starved larval third instar fat body of CS *Drosophila melanogaster*. These results are in line with the hypothesis which predicts overexpression of *MMP2* in starved samples compared to fed controls.

Experimental Errors

The collection and processing of samples consistently has the potential for experimental errors. One notable observation was the development of necrotic tissue in starved larvae during starvation experiments. This led to their exclusion

from dissection and RNA isolation. The presence of necrotic tissue could introduce variability in the samples, potentially affecting the RNA quality and subsequent gene expression analyses. While efforts were made to exclude affected larvae, the possibility of residual effects cannot be entirely ruled out.The RT-PCR and gel electrophoresis processes encountered several challenges, including smearing in gel lanes, amplification of only specific genes in certain samples, and primer dimer formation. These issues could have stemmed from factors such as DNA contamination, contamination of aliquots, and reduced primer efficiency. Issues like smearing in the lanes could make it difficult to interpret data. RT-qPCR results suggested that *MMP2* is overexpressed in a starved condition, even so there was lots of variability in the RT-qPCR results. Factors such as pipetting error, reaction conditions, or sample quality could contribute to this variability along with inherent variability in biological systems. Calculation of primer efficiencies is crucial for accurate quantification of gene expression using RT-qPCR. While reasonable primer efficiencies were observed for most genes, inconsistencies were noted in some cases. Variations in primer efficiency could affect the reliability of gene expression measurements. Despite these potential sources of experimental error, the overall trends observed in the data support the hypothesis. However, it is essential to acknowledge and address these sources of variability to ensure the reliability and validity of the experimental findings.

Conclusion and Future Directions

To conclude, the results of this study are consistent with the hypothesis that *MMP2* inhibits insulin signaling by degrading insulin receptor. *MMP2* transcript levels were higher in starved samples compared to fed controls in *Drosophila* third instar larval fat body. These findings are critical in understanding MMP2's role in insulin signaling during larval development. Overexpression of *MMP2* in a starved condition is consistent with the hypothesis that MMP2 regulates insulin signaling by degrading insulin receptor but it does not provide direct evidence for it. My research shows that *MMP2* is increased in response to starvation but does address whether or not MMP2 is, in fact, cleaving insulin receptor. In the future, it would be helpful to do experiments that understand the role of MMP2 in cleaving insulin receptor. A previous study showed in a murine model MMP14, a homolog for *Drosophila* MMP2, directly cleaved insulin receptor. They did this by performing western blot analysis of the β-chain protein of the insulin receptor. This allowed them to see suppression of insulin signaling resulting from MMP2 activity (Guo et al., 2022). A similar experiment could be conducted in *Drosophila* using specific antibodies for insulin receptor, which currently are not commercially available and would need to be generated in order to further examine the role of MMP2 in insulin signaling. Another way to examine the hypothesis that MPP2 degrades insulin receptor

could be to use a biomarker for autophagy such as Atg8a to measure the levels of autophagy and indirectly measure cleavage of insulin receptor. Another student in the Woodard Lab, Madigan Sticher, is working on this in her thesis. Alternatively, microscopy could be used to better understand early fat body remodeling in *Drosophila* fat body cells overexpressing *MMP2* to better understand the timeline of tissue remodeling and ECM degradation (Bond et al., 2011).

Studies of the effects of MMP2 on insulin signaling are impactful for the future of therapeutics for insulin insensitivity, metabolic dysfunction, and insulin-mediated cancers (Biglou et al., 2021). If MMP2 directly cleaves insulin receptor it may give insight into functional homologs of MMP2 in humans that could be used to develop therapeutics to modulate MMP2 activity if it is a major contributor to insulin insensitivity and metabolic dysfunction. The goal of this study was to better understand the mechanisms involved in *Drosophila* insulin signaling regulation. By doing this we hoped to gain a greater understanding of human diseases such as type 2 diabetes, high blood pressure, insulin insensitivity, other metabolic dysfunction, and other age associated pathologies. All of the data and results can assist in understanding the role of MMP2 in insulin signaling which could aid in advancing healthcare based research for insulin insensitivity and metabolic dysfunction.

Literature Cited

Álvarez-Rendón, Jéssica P., Rocío Salceda, and Juan R. Riesgo-Escovar. 2018. "Drosophila Melanogaster as a Model for Diabetes Type 2 Progression." *BioMed Research International* 2018 (April): 1417528. https://doi.org/10.1155/2018/1417528.

Anding, Allyson L., and Eric H. Baehrecke. 2015. "Chapter Three - Autophagy in Cell Life and Cell Death." In *Current Topics in Developmental Biology*, edited by Hermann Steller, 114:67–91. Apoptosis and Development. Academic Press. https://doi.org/10.1016/bs.ctdb.2015.07.012.

Aranda, Ana, and Angel Pascual. n.d. "Nuclear Hormone Receptors and Gene Expression | Physiological Reviews." Accessed March 31, 2024. https://journals.physiology.org/doi/full/10.1152/physrev.2001.81.3.1269?rfr_dat=cr_pub++0pubmed&url_ver=Z39.88-2003&rfr_id=ori%3Arid%3Acrossref.org.

Arquier, Nathalie, Charles Géminard, Marc Bourouis, Gisèle Jarretou, Basil Honegger, Alexandre Paix, and Pierre Léopold. 2008. "Drosophila ALS Regulates Growth and Metabolism through Functional Interaction with Insulin-Like Peptides." *Cell Metabolism* 7 (4): 333–38. https://doi.org/10.1016/j.cmet.2008.02.003.

Biglou, Sanaz G., William G. Bendena, and Ian Chin-Sang. 2021. "An Overview of the Insulin Signaling Pathway in Model Organisms *Drosophila Melanogaster* and *Caenorhabditis Elegans*." *Peptides* 145 (November): 170640. https://doi.org/10.1016/j.peptides.2021.170640.

Blanc, Richard. 1950. "*Biology of Drosophila* . M. Demerec, Ed. New York: Wiley; London: Chapman & Hall, 1950. 632 Pp. $10.00." *Science* 112 (2922): 794–794. https://doi.org/10.1126/science.112.2922.794.b.

Bond, Nichole D., Archana Nelliot, Marsha K. Bernardo, Melanie A. Ayerh, Kathryn A. Gorski, Deborah K. Hoshizaki, and Craig T. Woodard. 2011. "ßFTZ-F1 and Matrix Metalloproteinase 2 Are Required for Fat-Body Remodeling in Drosophila." *Developmental Biology* 360 (2): 286–96. https://doi.org/10.1016/j.ydbio.2011.09.015.

Bond, Nichole Dinell. n.d. “The Role of Ecdysone Signaling in Fat-Body Tissue Remodeling and Pupal Metabolism.” University of Nevada, Las Vegas. Accessed May 7, 2023. https://doi.org/10.34917/1453511.

Brew, Keith, and Hideaki Nagase. 2010. “The Tissue Inhibitors of Metalloproteinases (TIMPs): An Ancient Family with Structural and Functional Diversity.” *Biochimica et Biophysica Acta (BBA) - Molecular Cell Research* 1803 (1): 55–71. https://doi.org/10.1016/j.bbamcr.2010.01.003.

Buhler, Kurt, Jason Clements, Mattias Winant, Lenz Bolckmans, Veerle Vulsteke, and Patrick Callaerts. 2018. “Growth Control through Regulation of Insulin Signalling by Nutrition-Activated Steroid Hormone in Drosophila.” *Development* 145 (21): dev165654. https://doi.org/10.1242/dev.165654.

Chung, Henry, Tamar Sztal, Shivani Pasricha, Mohan Sridhar, Philip Batterham, and Phillip J. Daborn. 2009. “Characterization of Drosophila Melanogaster Cytochrome P450 Genes.” *Proceedings of the National Academy of Sciences of the United States of America* 106 (14): 5731–36. https://doi.org/10.1073/pnas.0812141106.

Cieplak, Piotr, and Alex Y. Strongin. 2017. “Matrix Metalloproteinases – From the Cleavage Data to the Prediction Tools and Beyond.” *Biochimica et Biophysica Acta (BBA) - Molecular Cell Research*, Matrix Metalloproteinases, 1864 (11, Part A): 1952–63. https://doi.org/10.1016/j.bbamcr.2017.03.010.

Colombani, Julien, Laurence Bianchini, Sophie Layalle, Emilie Pondeville, Chantal Dauphin-Villemant, Christophe Antoniewski, Clément Carré, Stéphane Noselli, and Pierre Léopold. 2005. “Antagonistic Actions of Ecdysone and Insulins Determine Final Size in *Drosophila*.” *Science* 310 (5748): 667–70. https://doi.org/10.1126/science.1119432.

Cui, Ning, Min Hu, and Raouf A. Khalil. 2017. “Biochemical and Biological Attributes of Matrix Metalloproteinases.” *Progress in Molecular Biology and Translational Science* 147: 1–73. https://doi.org/10.1016/bs.pmbts.2017.02.005.

Franz, Anna, Will Wood, and Paul Martin. 2018. “Fat Body Cells Are Motile and Actively Migrate to Wounds to Drive Repair and Prevent Infection.”

Developmental Cell 44 (4): 460-470.e3. https://doi.org/10.1016/j.devcel.2018.01.026.

Freeman, Andrew M., Luis A. Acevedo, and Nicholas Pennings. 2024. "Insulin Resistance." In *StatPearls*. Treasure Island (FL): StatPearls Publishing. http://www.ncbi.nlm.nih.gov/books/NBK507839/.

Goyal, Rajeev, Mayank Singhal, and Ishwarlal Jialal. 2024. "Type 2 Diabetes." In *StatPearls*. Treasure Island (FL): StatPearls Publishing. http://www.ncbi.nlm.nih.gov/books/NBK513253/.

Guo, Xuanming, Pallavi Asthana, Susma Gurung, Shuo Zhang, Sheung Kin Ken Wong, Samane Fallah, Chi Fung Willis Chow, et al. 2022. "Regulation of Age-Associated Insulin Resistance by MT1-MMP-Mediated Cleavage of Insulin Receptor." *Nature Communications* 13 (1): 3749. https://doi.org/10.1038/s41467-022-31563-2.

Hirabayashi, Susumu, Thomas J. Baranski, and Ross L. Cagan. 2013. "Transformed Drosophila Cells Evade Diet-Mediated Insulin Resistance Through Wingless Signaling." *Cell* 154 (3): 664–75. https://doi.org/10.1016/j.cell.2013.06.030.

Honegger, Basil, Milos Galic, Katja Köhler, Franz Wittwer, Walter Brogiolo, Ernst Hafen, and Hugo Stocker. 2008. "Imp-L2, a Putative Homolog of Vertebrate IGF-Binding Protein 7, Counteracts Insulin Signaling in Drosophila and Is Essential for Starvation Resistance." *Journal of Biology* 7 (3): 10. https://doi.org/10.1186/jbiol72.

Jia, Qiangqiang, Suning Liu, Di Wen, Yongxu Cheng, William G. Bendena, Jian Wang, and Sheng Li. 2017. "Juvenile Hormone and 20-Hydroxyecdysone Coordinately Control the Developmental Timing of Matrix Metalloproteinase–Induced Fat Body Cell Dissociation." *Journal of Biological Chemistry* 292 (52): 21504–16. https://doi.org/10.1074/jbc.M117.818880.

Kirk, Nicholas S., Qi Chen, Yingzhe Ginger Wu, Anastasia L. Asante, Haitao Hu, Juan F. Espinosa, Francisco Martínez-Olid, et al. 2022. "Activation of the Human Insulin Receptor by Non-Insulin-Related Peptides." *Nature Communications* 13 (1): 5695. https://doi.org/10.1038/s41467-022-33315-8.

Koetsier, Giron, and Eric Cantor. 2019. “A Practical Guide to Analyzing Nucleic Acid Concentration and Purity with Microvolume Spectrophotometers.” New England BioLabs Inc. chrome-extension://efaidnbmnnnibpcajpcglclefindmkaj/https://www.neb.com/en-us/-/media/nebus/files/application-notes/technote_mvs_analysis_of_nucleic_acid_concentration_and_purity.pdf?rev=c24cea043416420d84fb6bf7b554dbbb.

Nässel, Dick R., Olga I. Kubrak, Yiting Liu, Jiangnan Luo, and Oleh V. Lushchak. 2013. “Factors That Regulate Insulin Producing Cells and Their Output in Drosophila.” *Frontiers in Physiology* 4 (September): 252. https://doi.org/10.3389/fphys.2013.00252.

Notarangelo, Giulia. 2014. “The Genetic Control of Fat Body Development and Function in Drosophila Melanogaster.” South Hadley, MA: Mount Holyoke College. https://drive.google.com/drive/folders/0B6oNLL9CkRE9Q1IzdGJwMTdzTzg?resourcekey=0-adaEt8XOuiAv9Yq1WWOQdg.

Pagemccaw, A. 2008. “Remodeling the Model Organism: Matrix Metalloproteinase Functions in Invertebrates.” *Seminars in Cell & Developmental Biology* 19 (1): 14–23. https://doi.org/10.1016/j.semcdb.2007.06.004.

Papalexi, Efthymia. 2013. “The Genetic Control of Fat Body Development and Function in Drosophila Melanogaster.” South Hadley, MA: Mount Holyoke College. https://drive.google.com/drive/folders/0B6oNLL9CkRE9TU5lLWdIZ2tSOHM?resourcekey=0-QS-exPrg4TJmwXkJstT_Dw.

Pfaffl, Michael W. 2001. “A New Mathematical Model for Relative Quantification in Real-Time RT–PCR.” *Nucleic Acids Research* 29 (9): e45.

Rubin, Gerald M., Mark D. Yandell, Jennifer R. Wortman, George L. Gabor, Miklos, Catherine R. Nelson, Iswar K. Hariharan, et al. 2000. “Comparative Genomics of the Eukaryotes.” *Science* 287 (5461): 2204–15. https://doi.org/10.1126/science.287.5461.2204.

Semaniuk, Uliana, Veronika Piskovatska, Olha Strilbytska, Tetiana Strutynska, Nadia Burdyliuk, Alexander Vaiserman, Volodymyr Bubalo, Kenneth B. Storey, and Oleh Lushchak. 2021. “Drosophila Insulin-like

Peptides: From Expression to Functions – a Review." *Entomologia Experimentalis et Applicata* 169 (2): 195–208. https://doi.org/10.1111/eea.12981.

Semaniuk, Uliana V., Dmytro V. Gospodaryov, Khrystyna M. Feden'ko, Ihor S. Yurkevych, Alexander M. Vaiserman, Kenneth B. Storey, Stephen J. Simpson, and Oleh Lushchak. 2018. "Insulin-Like Peptides Regulate Feeding Preference and Metabolism in Drosophila." *Frontiers in Physiology* 9 (August): 1083. https://doi.org/10.3389/fphys.2018.01083.

Taguchi, Akiko, and Morris F. White. 2008. "Insulin-like Signaling, Nutrient Homeostasis, and Life Span." *Annual Review of Physiology* 70: 191–212. https://doi.org/10.1146/annurev.physiol.70.113006.100533.

Teleman, Aurelio A. 2010. "Molecular Mechanisms of Metabolic Regulation by Insulin in *Drosophila*." *Biochemical Journal* 425 (1): 13–26. https://doi.org/10.1042/BJ20091181.

Thummel, Carl S. 2001. "Molecular Mechanisms of Developmental Timing in *C. Elegans* and *Drosophila*." *Developmental Cell* 1 (4): 453–65. https://doi.org/10.1016/S1534-5807(01)00060-0.

Weigmann, Katrin, Robert Klapper, Thomas Strasser, Christof Rickert, Gerd Technau, Herbert Jäckle, Wilfried Janning, and Christian Klämbt. 2003. "FlyMove--a New Way to Look at Development of Drosophila." *Trends in Genetics: TIG* 19 (6): 310–11. https://doi.org/10.1016/S0168-9525(03)00050-7.

Yamanaka, Naoki, Kim F. Rewitz, and Michael B. O'Connor. 2013. "Ecdysone Control of Developmental Transitions: Lessons from *Drosophila* Research." *Annual Review of Entomology* 58 (1): 497–516. https://doi.org/10.1146/annurev-ento-120811-153608.

APPENDIX

Table 12. RT- qPCR 96 well plate layout *Actin 5C* and *MMP2*.

	1	**2**	**3**	**4**	**5**	**6**
A	Standard Curve 1/1 *Actin 5C*	Standard Curve 1/2 *Actin 5C*	Standard Curve 1/4 *Actin 5C*	Standard Curve 1/8 *Actin 5C*	Standard Curve 1/16 *Actin 5C*	Blank
B	Standard Curve 1/1 *MMP2*	Standard Curve 1/2 *MMP2*	Standard Curve 1/4 *MMP2*	Standard Curve 1/8 *MMP2*	Standard Curve 1/16 *MMP2*	Blank
C	Fed +RT *Actin 5C*	Fed +RT *Actin 5C*	Fed +RT *Actin 5C*	Fed -RT *Actin 5C*	Blank	Blank
D	Fed +RT *MMP2*	Fed +RT *MMP2*	Fed +RT *MMP2*	Fed -RT *MMP2*	Blank	Blank
E	Starved +RT *Actin 5C*	Starved +RT *Actin 5C*	Starved +RT *Actin 5C*	Starved -RT *Actin 5C*	Blank	Blank
F	Starved +RT *MMP2*	Starved +RT *MMP2*	Starved +RT *MMP2*	Starved -RT *MMP2*	Blank	Blank
G	Blank	Blank	Blank	Blank	Blank	Blank
H	Blank	Blank	Blank	Blank	Blank	Blank

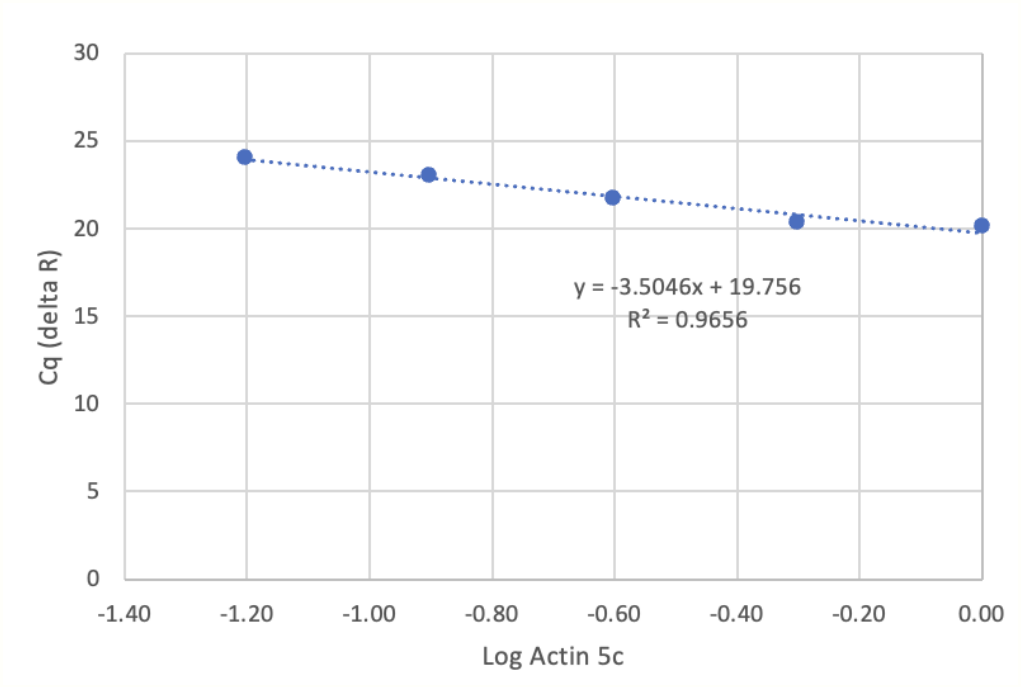

Figure 19. *Actin 5C* Standard Curve from 3/23/24 A. Depicts the log of the concentration of *Actin 5C* dilutions from CS whole larvae plotted against the C_q values. The slope is -3.5 and was used to calculate the *Actin 5C* primer efficiency which was found to be 1.93.

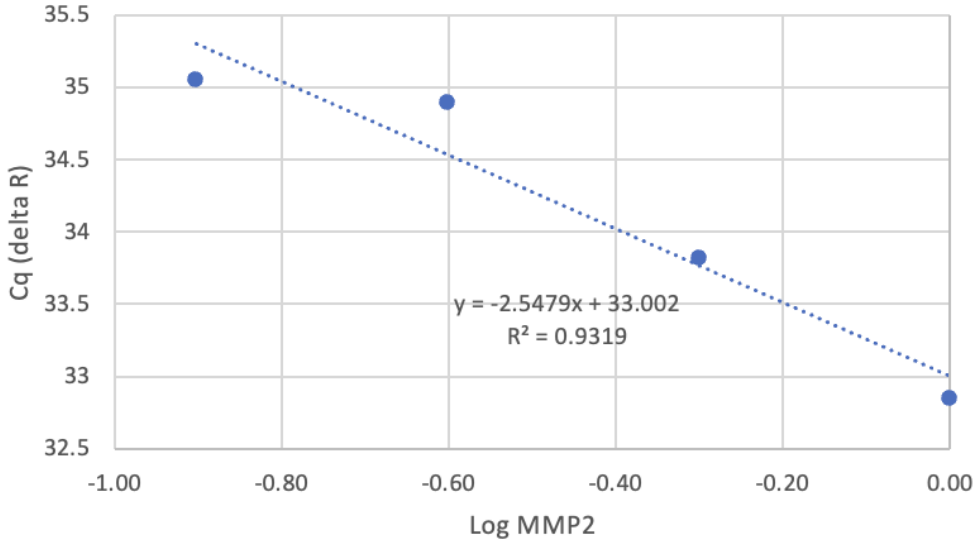

Figure 20. *MMP2* Standard Curve from 3/23/24 A. Depicts the log of the concentration of *MMP2* dilutions from CS whole larvae plotted against the C_q values. The slope is -2.55 and was used to calculate the *MMP2* primer efficiency which was found to be 2.47. Dilutions were excluded due to no C_q value being calculated during RT-qPCR, in this case missing 1/16 dilution.

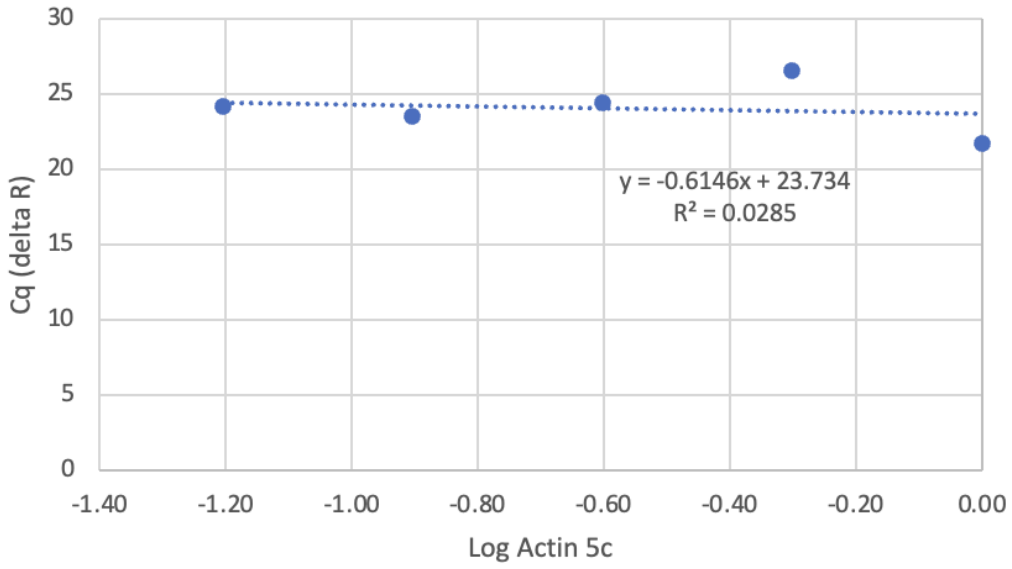

Figure 21. *Actin 5C* Standard Curve from 3/23/24 B. Depicts the log of the concentration of *Actin 5C* dilutions from CS whole larvae plotted against the C_q values. The slope is -0.61 and was used to calculate the *Actin 5C* primer efficiency which was found to be 42.37.

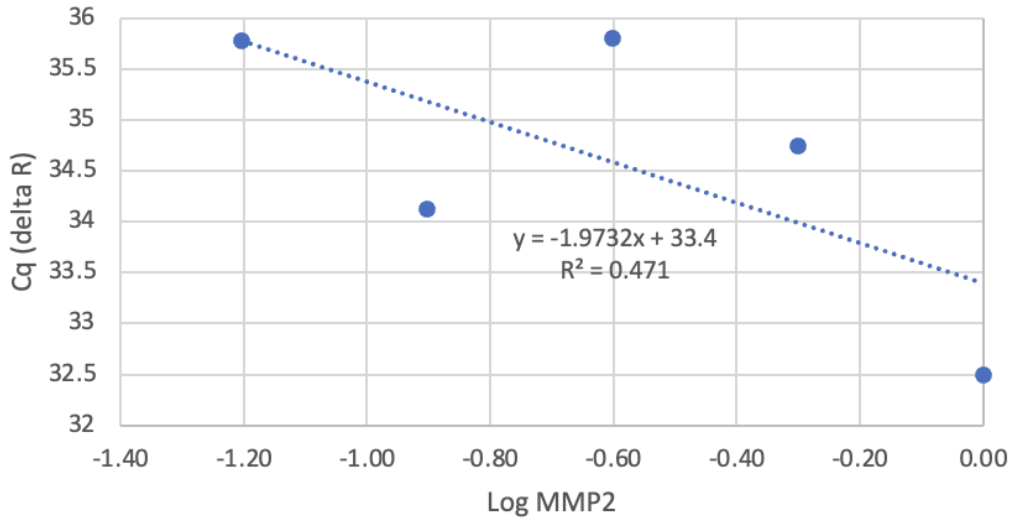

Figure 22. *MMP2* Standard Curve from 3/23/24 B. Depicts the log of the concentration of *MMP2* dilutions from CS whole larvae plotted against the C_q values. The slope is -1.97 and was used to calculate the *MMP2* primer efficiency which was found to be 3.21.

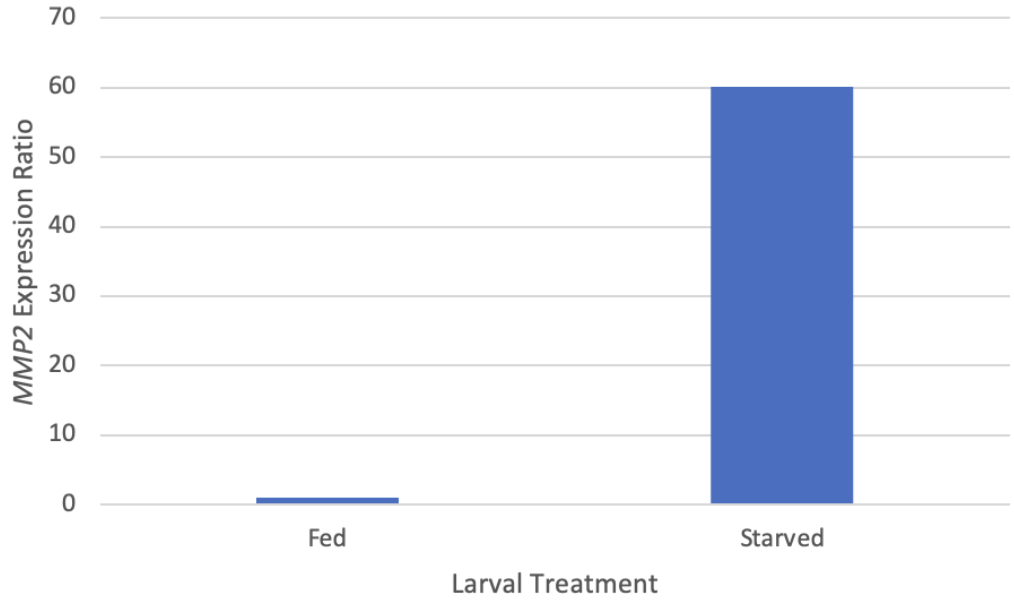

Figure 23. Expression Ratio of *MMP2* in Fed and Starved Feeding Third Instar Larval Fat Body of *Drosophila* for 3/19/24. The fed sample has a constant expression ratio of 1. The average starved expression ratio is 60.05.

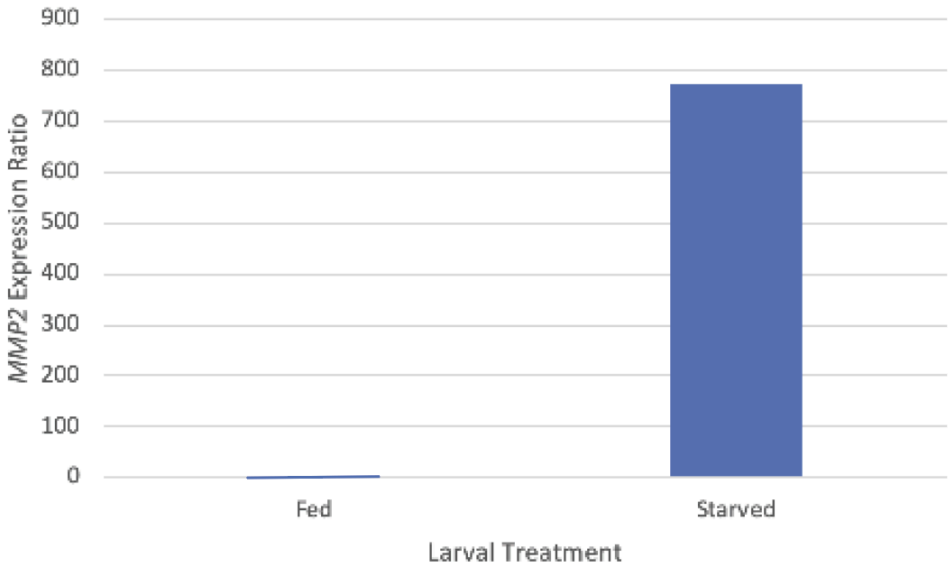

Figure 24. Expression Ratio of *MMP2* in Fed and Starved Feeding Third Instar Larval Fat Body of *Drosophila* for 3/23/24 A. The fed sample has a constant expression ratio of 1. The average starved expression ratio is 775.27.

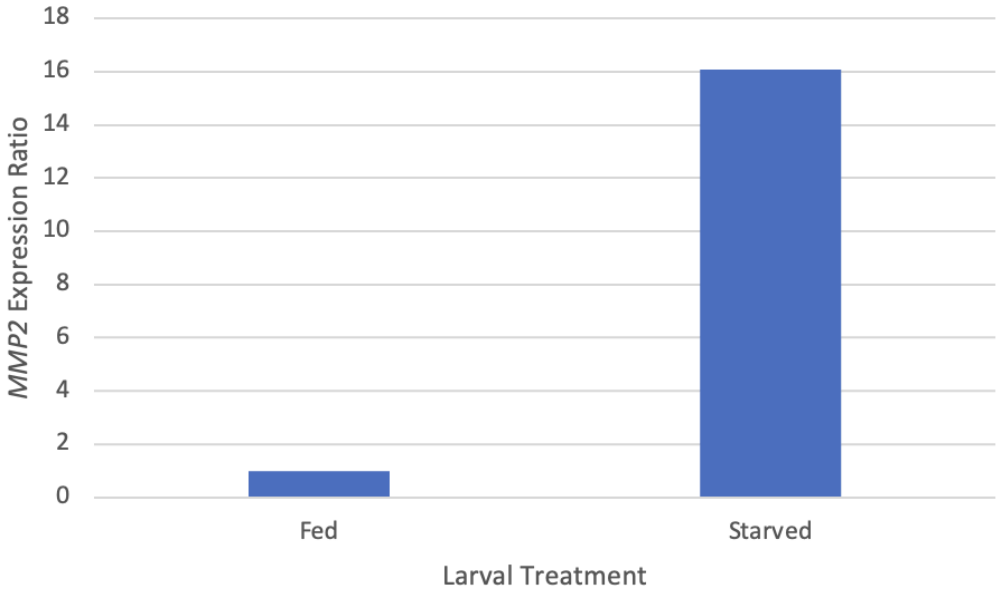

Figure 25. Expression Ratio of *MMP2* in Fed and Starved Feeding Third Instar Larval Fat Body of *Drosophila* for 3/23/24 B. The fed sample has a constant expression ratio of 1. The average starved expression ratio is 16.08.

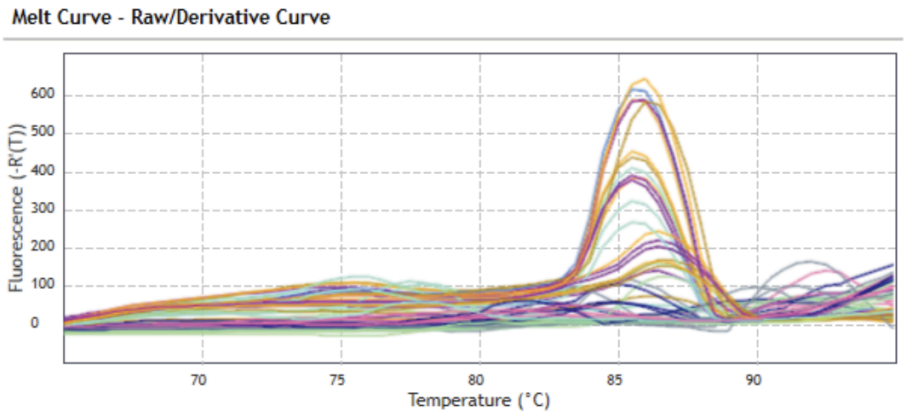

Figure 26. Melt Curve for RT-qPCR for 3/19/24. Melting curve shows there was no primer dimer in the sample. Melt curves were normal melting temperatures at around 80℃. This indicates that the fluorescence was due to full length PCR products and not primer dimer.

Table 13. List of Abbreviations.

Abbreviation	**Name**
AKT/PKB	Protein Kinase B
ANOVA	Analysis of Variance
APF	After Puparium Formation
bp	Base Pair
βFTZ-F1	Beta Fushi Tarazu
CS	Canton-S
C_q	Qualification cycle
dALS	*Drosophila* Insulin-like Growth Factor- Binding Protein Acid-Labile Subunit
dILP	*Drosophila* Insulin-Like Peptide
dInR	*Drosophila* Insulin Receptor
dFOXO	*Drosophila* Forkhead Box-containing Protein, O subfamily
ECM	Extracellular Matrix
ecdysone	20-Hydroxyecdysone
FOXO	Forkhead Box-containing Protein, O subfamily
GPI	Glycosylphosphatidylinositol
hINR	Human Insulin Receptor
IGF	Insulin Growth Factor
IGF-BP-ALS	Insulin-like Growth Factor-Binding Protein Acid-Labile Subunit
IGF-BP	Insulin-like Growth Factor-Binding Protein

IIS	Insulin-Like Growth Factor Signaling
ILPs	Insulin-like Peptides
Imp-L2	Imaginal Morphogenesis Protein-Late 2
InR	Insulin Receptor
IRS	Insulin Receptor Substrate
MMP	Matrix-metalloproteinase
MMP14	Matrix-metalloproteinase14
PAE	Predicted Aligned Error
PEPCK	Phosphoenolpyruvate carboxykinase
PIK3	Phosphatidylinositol 3-kinases
PIP2	Phosphatidylinositol 4,5-bisphosphate
PIP3	Phosphatidylinositol-triphosphate
PCR	Polymerase Chain Reaction
RT-PCR	Reverse Transcriptase Polymerase Chain Reaction
RT-qPCR	Real Time quantitative PCR
T2DM	Type 2 Diabetes Mellitus
TIMP	Tissue Inhibitors of Metalloproteinase
TOR	Target of Rapamycin